Journal of Paleontology, 98(5), 2024, p. 885–909

0022-3360/24/1937-2337
doi: 10.1017/jpa.2024.23

JOURNAL OF PALEONTOLOGY
A PUBLICATION OF THE Paleontological SOCIETY

The Late Miocene Plesiosoricidae and Soricidae (Eulipotyphla, Mammalia) from the Pannonian region, Slovakia

Florentin Cailleux,[1,2]* Lars W. van den Hoek Ostende,[2] and Peter Joniak[1]

[1]Comenius University in Bratislava, Faculty of Natural Sciences, Department of Geology and Paleontology, Ilkovičova 6, Mlynská dolina G, SK–842 15 Bratislava, Slovakia <cailleux1@uniba.sk>, <peter.joniak@uniba.sk>
[2]Naturalis Biodiversity Center, Darwinweg 2, 2333 CR Leiden, The Netherlands <lars.vandenhoekostende@naturalis.nl>

Non-technical Summary.—Soricidae (true shrews) is the largest modern family of insectivores. Already by the Late Miocene (from ca. 11.5 to ca. 5.5 million years), soricid faunas displayed a tendency to diversify. This is confirmed by the study of eight species of Soricidae from the Late Miocene of Slovakia, including one new genus. Additionally, we described one species of the extinct family Plesiosoricidae. Because of the increasing diversity of true shrews and the early record of several species, faunas from Slovakia confirm the key role of central Europe in the growth of this family during the Late Miocene. Furthermore, the large Slovak collections allowed us to gather new taxonomic information on previously reported species of Plesiosoricidae (*Plesiosorex evolutus*) and Soricidae (*Paenelimnoecus repenningi*, *Paenesorex bicuspis*, *Crusafontina endemica*, *Crusafontina kormosi*, *Amblycoptus jessiae*, *Asoriculus gibberodon*, *Petenyia dubia*), as well as on our newly named Soricidae, *Isterlestes aenigmaticus* n. gen. n. sp.

Abstract.—Soricidae is the most species-rich eulipotyphlan family since the Pliocene. Numerous Late Miocene soricids and plesiosoricids are well known from southern Europe. Localities from central Europe, despite being rare, historically have yielded better preserved material that reveals a great diversity. We here add to this existing record with the description of eight species from MN9- to MN12-aged localities of Slovakia (*Paenelimnoecus repenningi*, *Paenesorex bicuspis*, *Isterlestes aenigmaticus* n. gen. n. sp., *Crusafontina endemica*, *Crusafontina kormosi*, *Amblycoptus jessiae*, *Asoriculus gibberodon*, *Petenyia dubia*), alongside one species of Plesiosoricidae (*Plesiosorex evolutus*). The early occurrence of *A. gibberodon* and *A. jessiae*, the occurrence of *Paenesorex*, and the identification of *Isterlestes aenigmaticus* n. gen. n. sp., reinforce the hypothesis that the Pannonian region (south-eastern central Europe) was a source area for several soricid taxa (Allosoricinae, Anourosoricini, Soricini) during the Late Miocene.

UUID: https://zoobank.org/4466a6ea-4fc6-4a3b-88f8-dbe020f2292d

Introduction

The late Neogene was a period of consequential change in the familial composition of Eulipotyphla. The shrew-like family Plesiosoricidae is last recorded in the Vallesian of central Europe, and both the Dimylidae and the Heterosoricidae families went extinct during the early Turolian, after a short period of apparent recovery. Despite periods of relative stability, the Erinaceidae also show a slow decline during the Late Miocene. At the same time, the Talpidae were momentarily diverse, mainly thanks to the success of weakly contested niches, namely the ones occupied by fossorial and semiaquatic taxa (Ziegler, 2006a, b; Cailleux et al., 2024). It is still unclear to what extent changes in the dynamics of these eulipotyphlan families affected other small mammal taxa, but it seems that the diversity of Eulipotyphla species is mainly restricted by the number of accessible niches (Van den Hoek Ostende et al., 2019). Regardless, the Late Miocene witnessed progressive flourishing of the Soricidae, now the fourth largest mammal family in terms of specific diversity (Burgin et al., 2018).

Although the Pliocene is usually seen as the "era of shrews," it is questionable if the explosion of shrew diversity in the Pliocene is actually an unfortunate consequence of the limited number of Late Miocene, and especially latest Miocene, European localities. Most of these localities are situated in southern Europe, and especially in Spain (The NOW Community, 2023). However, these regions correspond to sink areas (e.g., Van Dam, 2004). Namely, records from these areas are often peripheral occurrences of generalist species, and thus represent only a fraction of the diversity found in regions with more humid and stable environments, notably central Europe (Furió et al., 2011).

Central Europe was an area of high insectivore diversity during the Late Miocene (Ziegler, 2006b; Furió et al., 2011). This also applies to the Soricidae despite two main limiting factors: (1) the small number of latest Miocene localities, where soricid faunas are expected to be richer; and (2) the fragmented

*Corresponding author

nature of soricid fossils, making taxonomic identifications difficult for the numerous generalist and small-sized taxa. This paper aims to fill part of that gap by describing the Soricidae from several rich Late Miocene localities ranging from MN9 to MN12. It is part of a series describing the insectivore and bat faunas from the Late Miocene of Slovakia (Cailleux et al., 2023, 2024). In addition, the Plesiosoricidae of these localities are described. Finally, we briefly discuss the faunal change occurring in the eulipotyphlan community during the Late Miocene, which resulted in the disappearance of Plesiosoricidae and the progressive success of Soricidae.

Material and methods

The present work describes materials extracted from six Late Miocene Slovak localities: Borský Svätý Jur (MN9); Studienka A, D, and E (MN9); Pezinok (MN10); Triblavina (MN11); Krásno (MN11); and Šalgovce 4 and 5 (MN12) (ages according to Joniak, 2005, 2016; Šujan et al., 2016; Joniak and Šujan, 2020; Sabol et al., 2021; Cailleux et al., 2023). These sites are located in the Vienna and Danube basins. The geological setting has been summarized by Cailleux et al. (2023).

The material described here consists of 681 specimens, including 679 Soricidae and 2 Plesiosoricidae. The dental terminology of plesiosoricids is not yet stabilized. We here are following the dental terminology of Van Valen (1966). Additionally, the cuspules found labially to the paracone and metacone are called parastylocone and metastylocone, respectively. The figured upper dentition has been annotated to make these structures more easily recognizable in future works. The measurement protocol derives from Schötz (1989). The dental terminology and measurement protocol of soricids is somewhat stable, with most authors (e.g., Mészáros, 1996; Van Dam, 2004; Furió, 2007; Minwer-Barakat et al., 2010; Hugueney et al., 2012; Rzebik-Kowalska and Rekovets, 2016) referring to Reumer (1984). In the mentioned works, slight differences are sometimes found with the original terminology of Reumer (1984), especially regarding the entocristid (entoconid crest in Reumer, 1984) and the oblique cristid (oblique crest in Reumer, 1984). These slight differences, formulated by Van den Hoek Ostende (2001), are followed here (Fig. 1). In addition, for both plesiosoricids and soricids, we follow Zazhigin and Voyta (2022) in the use of the terms pre-/postparacrista, and pre-/postmetacrista. We also use the terms preprotocrista and postprotocrista to refer to the crest found anteriorly and posteriorly to the protocone, respectively (Fig. 1). Finally, we retain the abbreviation BL (buccal length) used in Reumer (1984) to refer to the labial length.

All measurements are given in millimeters (mm). The dental elements were measured using a digital measuring microscope (Eakins 37MP) with a mechanical stage and digital measuring clocks (Mitutoyo 350-352-30). The identification numbers, laterality, and measurements of specimens are provided in Supplemental Data 1. Specimens in figures are represented in left orientation. Reversed specimens are indicated by an underlined number. Unless otherwise noted, SEM pictures are in occlusal view. Drawings were obtained with a graphic tablet (Wacom Intuos Pro) and the software Autodesk SketchBook (v. 8.7.1; https://www.sketchbook.com/). All the described specimens are housed at the Department of Geology and Paleontology, Comenius University, Bratislava.

List of abbreviations.—AW, anterior width; BL, labial (buccal) length; H, height; L, length; LL, lingual length; LT, length of the talon; N, number of specimens; PE, length of the posterior emargination; PW, posterior width; TAW, talonid width; TRW, trigonid width; W, width.

List of localities.—BJ, Borský Svätý Jur; KR, Krásno; RC, recent; SG, Šalgovce; ST, Studienka; TB, Triblavina.

Repositories and institutional abbreviations.—AMPG, Athens Museum of Palaeontology and Geology, Greece; ICP, Institut Català de Paleontologia Miquel Crusafont, Spain; MÁFI, Hungarian Geological Institute, Hungary; NHMA, Natural History Museum of Augsburg, Germany; NHMW, Natural History Museum of Vienna, Austria.

Systematic paleontology

Order Eulipotyphla Waddell, Okada, and Hasegawa, 1999
Family Plesiosoricidae Winge, 1917
Subfamily Plesiosoricinae Winge, 1917
Genus *Plesiosorex* Pomel, 1848

Type species.—*Plesiosorex soricinoides* (de Blainville, 1838).

Other referred species.—*Plesiosorex styriacus* (Hofmann, 1892); *P. latidens* (Hall, 1929); *P. germanicus* (Seemann, 1938); *P. coloradensis* Wilson, 1960; *P. schaffneri* Engesser, 1972; *P. donroosai* Green, 1977; *P. aydarlensis* Kordikova, 2000; *P. roosi* Franzen, Fejfar, and Storch 2003; *P. greeni* Martin and Lim, 2004; *P. evolutus* Ziegler, 2006a; *P. martinii* Engesser and Storch, 2008; *P. fejfari* Oshima, Tomida, and Orihara, 2017; *P. shanqini* Li, 2022.

Diagnosis.—See Gunnell et al. (2008, p. 112).

Occurrence.—*Plesiosorex* is a widespread genus identified from the late Oligocene to Late Miocene of Europe and the Miocene of North America and Asia (e.g., Schötz, 1989; Gunnell et al., 2008; Li, 2022).

Plesiosorex evolutus Ziegler, 2006
Figure 2

Holotype.—Right M1, NHMW 2004z0182/0001, Schernham, Austria (Ziegler, 2006a).
H = 0.83

Diagnosis.—See Ziegler (2006a, p. 109).

Occurrence.—MN9 and MN10 of Austria (Ziegler, 2006a) and MN9 of Slovakia (this paper).

Description.—The M1 is a stout and rectangular element (Fig. 2.1). A low and wide postmetacrista connects the

https://doi.org/10.1017/jpa.2024.23 Published online by Cambridge University Press

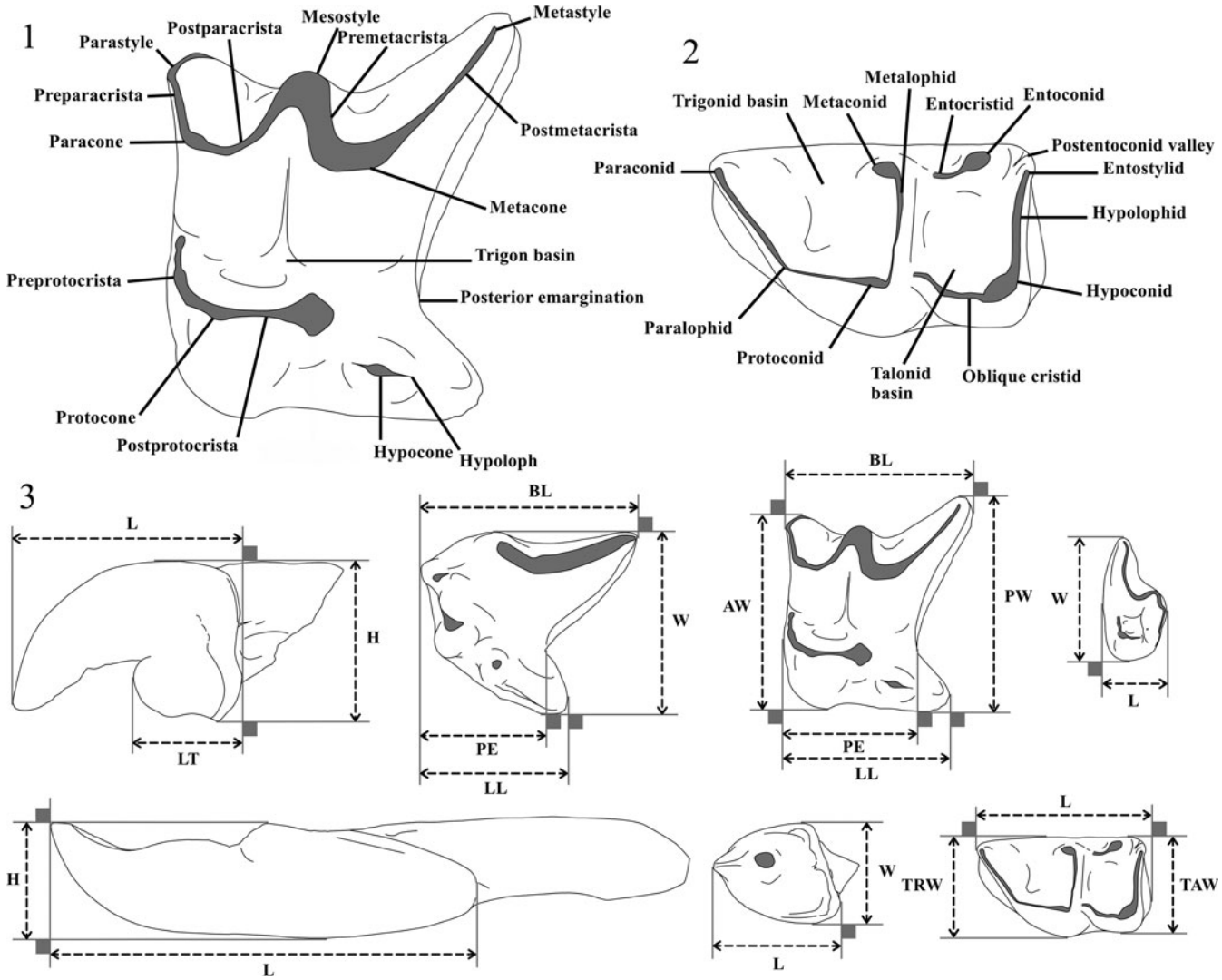

Figure 1. Terminology used for the (**1**) M1 and (**2**) m1 of Soricidae, and (**3**) measurements protocol for I1, P4, M1, M3, i1, p4 and m1. AW = anterior width; BL = labial (buccal) length; H = height; L = length; LL = lingual length; LT = length of the talon; N = number of specimens; PE = length of the posterior emargination; PW = posterior width; TAW = talonid width; TRW = trigonid width; W = width.

metacone to the posterolabial corner. The premetacrista is short. The metastylocone is weakly connected to the robust parastylocone. The latter is as high as the paracone. The labial basin is large and almost entirely closed. The anterolabial extension bears a distinct parastyle, included in a thin and curved crest starting from the base of the parastylocone and ending anterior to the paracone. This configuration creates a small anterolabial depression, as the postparacrista is short. The protocone is connected to the paracone and to the metaconule. The preprotocrista is high. The hypocone is connected to the metaconule by a low ridge. The hypoloph is enlarged. There is a premetaconule crest but no postmetaconule crest. Instead, there is a discontinuous succession of small irregularities (Fig. 2.1). Short anterior and lingual cingula are present.

The p4 has a high conical protoconid from which a sharp and straight paralophid extends. The paraconid is low. A robust and sharp posterior centrocristid connects the protoconid to the posterior margin, splitting the proto-talonid into two small basins (Fig. 2.2).

Material.—Borský Svätý Jur: one M1 (L = 5.28; W = 3.89), one fragment of p4 (L = ~3.11).

Remarks.—The combination of a heavy metastylocone and the lack of clear postmetaconule crest on M1 is found in a single species of *Plesiosorex*, *P. evolutus*. The size of the M1 is intermediate between the specimen from Götzendorf (MN9) and the one from Schernham (MN10). Overall, our M1 is morphologically similar to the holotype from Schernham (Ziegler, 2006a), but differs from it by the presence of crests around the hypocone, which is an ancestral character found in the European Middle Miocene species *P. germanicus* and *P. schaffneri* (see Viret, 1940; Engesser, 1972). Such intermediate features can be expected since Borský Svätý Jur is now the oldest occurrence of *P. evolutus*. The progressive

https://doi.org/10.1017/jpa.2024.23 Published online by Cambridge University Press

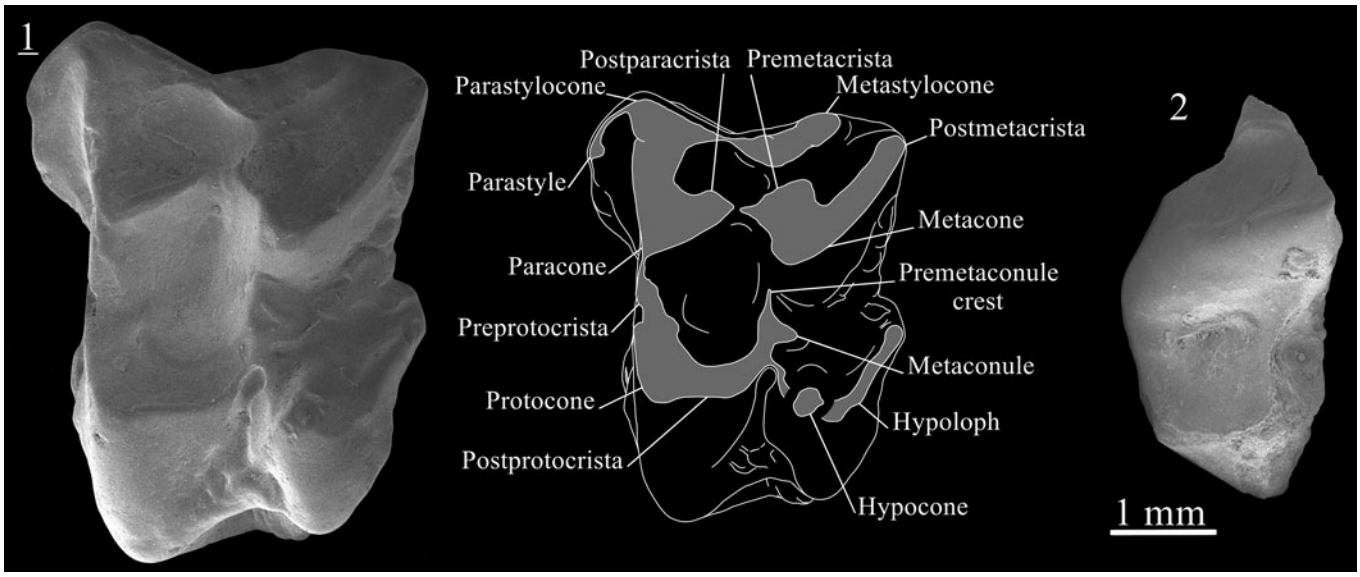

Figure 2. Scanning electron photomicrographs of *Plesiosorex evolutus* from Borský Svätý Jur. (**1**) M1, BJ213480, with explanatory drawing; (**2**) fragment of p4, BJ213480. Image with underlined number is reversed.

oblique elongation of the hypoconal basin and the development of the buccal conules confirm the strong phylogenetic relationship between *P. germanicus* and *P. evolutus*, as reconstructed by Li (2022, fig. 4).

Family Soricidae Fischer, 1814
Subfamily Allosoricinae Fejfar, 1966
Genus *Paenelimnoecus* Baudelot, 1972

Type species.—*Paenelimnoecus crouzeli* Baudelot, 1972.

Other referred species.—*Paenelimnoecus pannonicus* (Kormos, 1934); *P. micromorphus* (Doben-Florin, 1964); *P. repenningi* Bachmayer and Wilson, 1970; *P. truyolsi* Gibert, 1975; *P. obtusus* Storch, 1995; *P. chinensis* Jin and Kawamura, 1997.

Diagnosis.—See Baudelot (1972, p. 100).

Occurrence.—*Paenelimoecus* is recorded from the Early Miocene to Pliocene of Europe (Baudelot, 1972; Reumer, 1984; Pipík and Sabol, 2005; Ziegler, 2006a; Van den Hoek Ostende et al., 2009) and Middle Miocene to Pliocene of Asia (Engesser, 1980; Storch, 1995; Jin and Kawamura, 1997; Furió et al., 2014).

Paenelimnoecus repenningi (Bachmayer and Wilson, 1970)
Figure 3.1–3.6

Holotype.—Fragment of left mandible, NHMW 1970/1388, Kohfidisch, Austria (Bachmayer and Wilson, 1970).

Diagnosis.—See Bachmayer and Wilson (1970, p. 549), under the name *Petenyiella*? *repenningi*.

Occurrence.—From MN9 to MN12 of Europe (Bachmayer and Wilson, 1970; Ziegler, 2005, 2006a; Furió, 2007).

Description.—A few dental specimens from Studienka A and Triblavina show a darker stain on their tips.

The I1 is a strongly procumbent element with only a slightly curved dorsal margin (Fig. 3.1). The talon is weak and bears a pointy labial cuspule. A marked crest is present on the lingual flank of the talon, continuing along the crown. The labial cingulum is strong.

The M1 has high labial crests and deep ectoloph, creating a clear W-shaped complex (Fig. 3.2). The mesostyle is intermediate in height between the low metastyle and the moderately high parastyle. The lingual complex is low. The broad protocone is connected to the anterolingual base of the paracone by a curved preprotocrista. The postprotocrista is straight and ends free lingual to the metacone. The posterolingual extension is narrow because of the deep posterior emargination. The hypocone is reduced and included in a crest joining the posterior cingulum. The M2 is barely distinguishable from the M1: the postmetacrista is more compressed and the posterolingual extensions are slightly less extended.

The i1 is slender and bicuspulate. The a1 is an ovoid, exaenodont and flat premolar with a cuspid in anterior position. An oblique crest is present posterior to this cuspid. The lingual, posterior, and labial margin are surrounded by a continuous cingulid.

The m1 has a laterally compressed trigonid with a bi-partitioned paralophid (Fig. 3.5). The paraconid is lower than the metaconid. The metalophid is high. The hypoconid is laterally compressed. The oblique cristid joins the trigonid wall below the protoconid. The entoconid is vestigial and independent. The hypolophid is straight. The postentoconid valley is narrow. Continuous anterior and labial cingula are present. The m2 has the same length as the m1 but has wider trigonid and talonid and a protoconid in a more labial position. The m3 is a small molar with reduced talonid. On the trigonid, the paralophid is curved and the metaconid is lower than the projected paraconid. The talonid displays a single cuspid, connected to the trigonid wall by a short crest. A short lingual swelling is

https://doi.org/10.1017/jpa.2024.23 Published online by Cambridge University Press

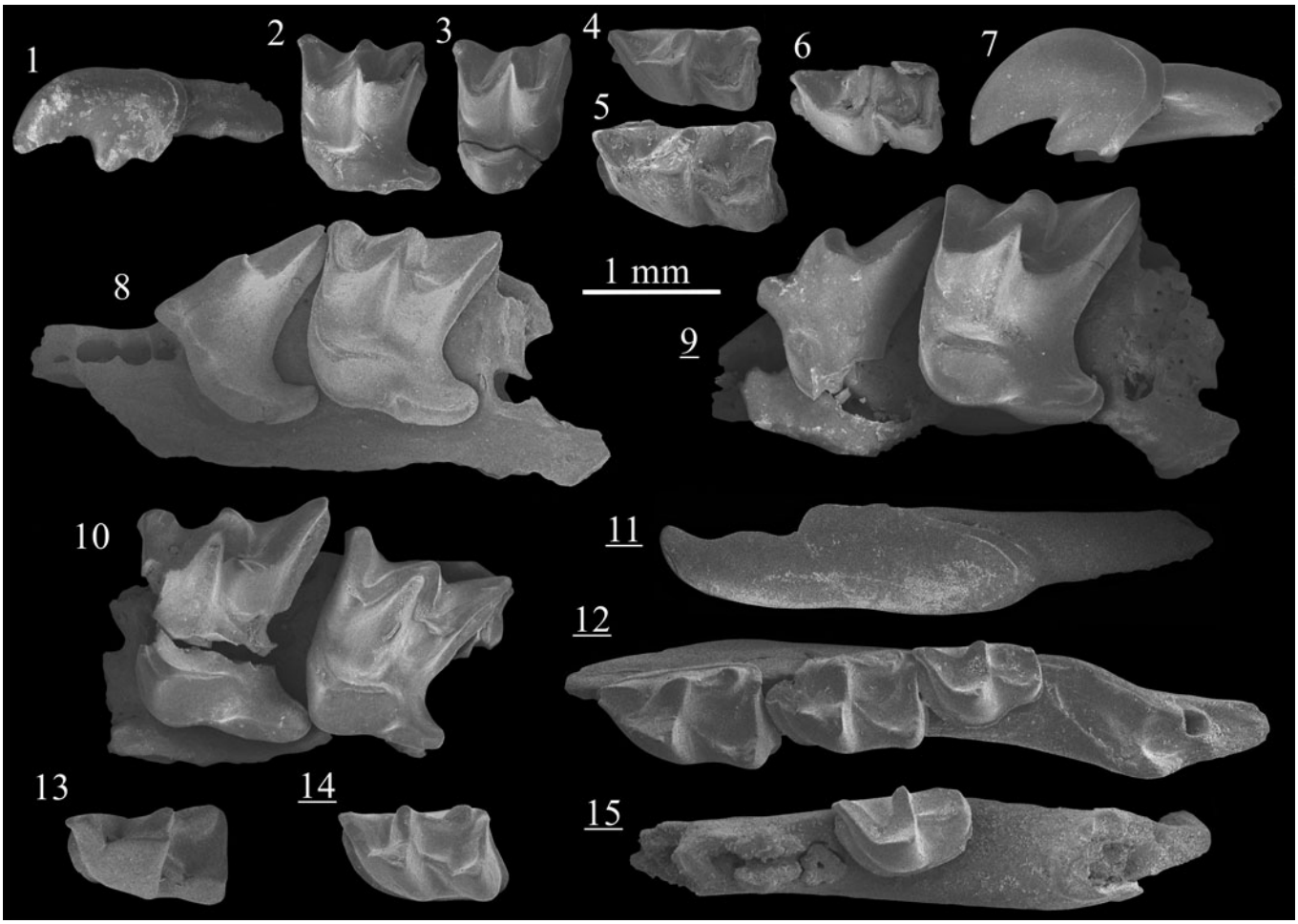

Figure 3. Scanning electron photomicrographs of *Paenelimnoecus repenningi* from (**1–3**) Studienka A and (**4–6**) Krásno, and (**7–15**) *Paenesorex bicuspis* from Borský Svätý Jur. (**1**) I1, ST214432, labial view; (**2**) M2, ST214433; (**3**) M2, ST214436; (**4**) m1, KR127304; (**5**) m1, KR127306; (**6**) m2, KR127305; (**7**) I1, BJ213704, labial view; (**8**) fragment of maxillary with P4–M1, BJ213719; (**9**) fragment of maxillary with P4–M1, BJ213720; (**10**) fragment of maxillary with M1–M2; (**11**) i1, BJ213766, labial view; (**12**) fragment of mandible with m1–m3, BJ213771; (**13**) m1, BJ213777; (**14**) m2, BJ213790; (**15**) fragment of mandible with m3, BJ213787. Images with underlined numbers are reversed.

attached to the cuspid, leading to a triangular shaped dental wear in occlusal view.

Material.—Studienka A: four I1 (L = 1.23, LT = 0.66, H = 0.80; L = 1.21, LT = 0.65, H = 0.78; L = 1.10, LT = 0.51, H = 0.77; L = 1.20, LT = 0.61, H = 0.72), two M1 (BL = 0.89, TRW = 0.97; BL = 0.98), three M2 (BL = 1.03, PE = 0.77, LL = 0.99, TRW = 1.15, TAW = 1.16; BL = 0.87, PE = 0.79, TRW = 1.11; BL = 1.00), one i1 (H = 0.50), two m1 (TRW = 0.57; TRW = 0.55, TAW = 0.60), one m3 (L = 0.84, W = 0.52).

Triblavina: two I1 (L = 1.41, LT = 0.65, H = 0.92), two i1 (L = 2.66; L = 2.18), one m2 (TRW = 0.59).

Krásno: two I1 (H = 1.01; H = 0.83), one fragment of M1, one M2 (BL = 1.00, PE = 0.82), two i1 (H = 0.64), one a1 (L = 0.92, W = 0.67), five m1 (L = 1.06, TRW = 0.56, TAW = 0.59; L = 1.10, TRW = 0.58, TAW = 0.59; L = 1.09, TRW = 0.59, TAW = 0.63), two m2 (L = 1.10, TRW = 0.63, TAW = 0.65; TAW = 0.83).

Remarks.—The combination of moderately elongated paralophid, lack of entocristid, and vestigial entoconid on lower molars is a clear indication of *Paenelimnoecus*. Few features, namely, the position of the mental foramen and the progressive reduction of the entoconid, distinguish the European Miocene species *P. crouzeli* (MN6–MN9), *P. repenningi* (MN9–MN12), and *P. pannonicus* (MN13–MN17). In our samples, there is no entocristid but a still visible entoconid, which fits the evolutionary degree of *P. repenningi*. This species was originally distinguished from *P. pannonicus* by its larger size (Bachmayer and Wilson, 1970), but most samples of *P. repenningi* have smaller dimensions than those found at the type locality of Kohfidisch (see Ziegler, 2006a). This is also apparent in our material.

The mean measurements of *Paenelimnoecus* species (Table 1) highlight a trend toward the narrowing/elongation of m1. The Lm1/Wm1 ratio, which is between 1.56 and 1.71 for the Early and Middle Miocene species (*P. micromorphus*, *P. truyolsi*, and *P. crouzeli*) and between 1.65 and 2.05 for the Late Miocene species (*P. repenningi*, *P. pannonicus, P. obtusus*, *P. chinensis*), appears to be a good proxy to test the validity of several specific attributions.

https://doi.org/10.1017/jpa.2024.23 Published online by Cambridge University Press

Table 1. Mean measurements (in mm) of the lower molars of *Paenelimnoecus*, *Viretia*, and *Allosorex* species. Data from to Fejfar (1966), Engesser (1980), Crochet and Green (1982), Reumer (1984), Storch (1995), Mészáros (1996, 1998b, 1999), Jin and Kawamura (1997), Ziegler (2005, 2006a), Furió (2007), Rzebik-Kowalska and Lungu (2009), Minwer-Barakat et al. (2010), Hugueney et al. (2012), Prieto and Van Dam (2012), Furió et al. (2014), Fejfar et al. (2020).

Species	Localities	MN units	Lm1	Wm1	Lm2	Lm3	Lm1/Wm1	Lm1/Lm2	Lm1/Lm3
P. micromorphus	Petersbuch 28	MN3/4	0.99	0.58	0.98	0.76	**1.71**	1.01	1.30
P. micromorphus	Petersbuch 2	MN4	0.94	0.56	1.03	0.76	**1.68**	0.91	1.24
P. micromorphus	Vieux-Collonges	MN5	1.13	0.68	1.11	0.93	**1.66**	1.02	1.22
P. truyolsi	Villafeliche 4A	MN5	1.03	0.66	0.93	—	**1.56**	1.11	—
P. truyolsi	Villafeliche 4B	MN5	—	—	1.05	0.82	—	—	—
P. truyolsi	Moratilla 2	MN5	1.08	0.66	1.01	0.93	**1.64**	1.07	1.16
P. crouzeli	Sansan	MN6	1.14	0.67	1.14	0.86	**1.70**	1.00	1.33
P. crouzeli	La Grive L7	MN7/8	1.05	0.64	1.02	0.64	**1.64**	1.03	1.64
P. crouzeli	La Grive M	MN7/8	1.02	0.64	0.96	0.75	**1.59**	1.06	1.36
Paenelimnoecus sp. 1	Eskihisar	MN7/8	1.08	0.66	—	—	**1.64**	—	—
Paenelimnoecus sp. 2	Eskihisar	MN7/8	1.16	0.74	1.18	0.87	**1.57**	0.98	1.33
P. aff. *P. repenningi*	Rudabánya	MN9	1.12	0.66	1.09	0.81	**1.70**	1.03	1.38
P. repenningi	Richardhof-Golfplatz	MN9	1.22	0.61	1.14	—	**2.00**	1.07	—
P. repenningi	Montredon	MN10	1.03	0.62	1.04	0.97	**1.66**	0.99	1.06
P. repenningi	Sümeg	MN10	—	—	1.11	1.02	—	—	—
P. repenningi	Richardhof-Wald	MN10	1.05	0.57	1.06	0.88	**1.84**	0.99	1.19
P. repenningi	Kohfidisch	MN11	1.19	0.65	1.13	0.84	**1.83**	1.05	1.42
P. repenningi	Eichkogel	MN11	1.09	0.59	1.11	0.83	**1.85**	0.98	1.31
P. repenningi	Krásno	MN11	1.08	0.60	1.10	—	**1.80**	0.98	—
P. repenningi	Csákvár	MN11	1.25	0.61	1.11	0.97	**2.05**	1.13	1.29
P. repenningi	Tardosbánya	MN12	1.19	0.65	1.14	0.83	**1.83**	1.04	1.43
P. repenningi	Polgárdi 4	MN13	1.23	0.72	1.18	0.90	**1.71**	1.04	1.37
P. cf. *P. repenningi*	Fortuna	MN13	1.04	0.57	1.02	—	**1.82**	1.02	—
Paenelimnoecus sp.	Hayranlı	MN10–11	1.07	0.65	—	—	**1.65**	—	—
P. obtusus	Ertemte	MN13	1.13	0.67	1.04	0.85	**1.69**	1.09	1.33
P. pannonicus	Tollo de Chiclana 1B	MN15	1.14	0.61	1.09	—	**1.87**	1.05	—
P. pannonicus	Tollo de Chiclana 1	MN15	1.13	0.56	—	—	**2.02**	—	—
P. pannonicus	Csarnota 2	MN15	1.2	0.66	1.10	0.77	**1.82**	1.09	1.56
P. pannonicus	Tollo de Chiclana 13	MN16	1.13	0.66	—	—	**1.71**	—	—
P. pannonicus	Tollo de Chiclana 3	MN16	1.14	0.68	1.12	0.85	**1.68**	1.02	1.34
P. pannonicus	Osztramos 7	MN16	1.12	0.68	0.98	0.66	**1.65**	1.14	1.70
P. chinensis	Yinan	MN16	1.2	0.65	1.12	—	**1.85**	1.07	—
"*P. repenningi*"	Cobruci	MN11	1.08	0.76	—	—	**1.42**	—	—
V. gracilidens	Oberdorf 4	MN4	1.52	0.87	1.49	1.28	**1.75**	1.02	1.19
V. gracilidens	Devínska Nová Ves - Štokeravská vápenka	MN6	1.5	0.95	1.22	0.98	**1.58**	1.23	1.53
V. gracilidens	Giggenhausen	MN7/8	1.5	0.80	—	—	**1.88**	—	—
V. gracilidens	La Grive	MN7/8	1.57	0.81	1.46	0.98	**1.94**	1.08	1.60
"*A.* cf. *A. stenodus*"	Alsótelekes	MN9	2.08	0.98	1.68	—	**2.12**	1.24	—
A. stenodus	Ivanovce	MN15	2.70	0.98	1.99	1.08	**2.76**	1.36	2.50

The Lm1/Wm1 ratio of the single m1 of *P. repenningi* from MN11 of Čobruci, Moldova, equals 1.42 (based on Rzebik-Kowalska and Lungu, 2009). This is lower than all material attributed to the genus. The figured specimen (Rzebik-Kowalska and Lungu, 2009, fig. 9, F2) also displays a strong entoconid, leaving doubts about the taxonomic identification. Apart from this material, the lowest ratio in the Late Miocene of Europe (1.70) is found in *P.* aff. *P. repenningi* from MN9 of Rudabánya, described by Ziegler (2005). The use of open nomenclature was motivated by the intermediate morphology of the sample, between *P. crouzeli* and *P. repenningi*. The Lm1/Wm1 ratio is found within a very narrow overlapping area of the two species, supporting that the species from Rudabánya is a transitional form.

The Lm1/Wm1 ratio of *Paenelimnoecus* sp. 1 from Eskihisar (MN7/8, Anatolia; Engesser, 1980) equals 1.64, which fits the data obtained from *P. crouzeli*. *Paenelimnoecus* sp. 2 from Eskihisar has a slightly lower ratio (1.57), but its large size distinguishes it from other known Early and Middle Miocene species. *Paenelimnoecus* sp., described from MN10–11 of Hayranlı (Furió et al., 2014), has a Lm1/Wm1 ratio (1.65), which is significantly smaller than other Late Miocene species. This suggests that *Paenelimnoecus* sp. 1 from Eskihisar and *Paenelimnoecus* sp. from Hayranlı are closely related.

The subfamilial allocation of *Paenelimnoecus* is unstable (see Baudelot, 1972; Reumer, 1984, 1992; Storch, 1995; Fefjar et al., 2006, 2020; Engesser, 2009; Van den Hoek Ostende et al., 2009; Hugueney et al., 2012). Its exclusion from Allosoricinae by Fejfar et al. (2006), Hugueney et al. (2012), and Prieto and Van Dam (2012) was motivated by the lack of carnassial development on lower molars, which is a diagnostic feature of *Allosorex stenodus* Fejfar, 1966, that already had been recorded in the Middle Miocene species *Viretia* ("*Allosorex*") *gracilidens* (Viret and Zapfe, 1952). However, except for the carnassial, there are few shared features between *Viretia* and *Allosorex*. Both taxa are also separated by a large stratigraphic gap, from MN7/8 to MN15 (ca. 8 my). *Allosorex* cf. *A. stenodus* has been identified in the MN9 of Alsótelekes (Hungary; Mészáros, 1999), but the three identified specimens actually show strong morphometrical and morphological similarities with early *Crusafontina*. On the other hand, Table 1 shows that the Late Miocene species of *Paenelimnoecus* acquired narrower m1, which is a feature concomitant with the development of carnassial molar.

Fundamentally, the instability of the subfamily Allosoricinae is caused by the highly specialized *Allosorex stenodus*. The rare adaptation to a specialized diet in a lineage should not justify the exclusion of older taxa that constitute convenient

https://doi.org/10.1017/jpa.2024.23 Published online by Cambridge University Press

structural ancestors. The subfamily Paenelimnoecinae Fejfar, Storch, and Tobien, 2006, appears unsupported because it is defined by the non-presence of such dietary specialization. Despite the small size and lack of trigonid elongation, the presence of narrower lower molars, with the reduction of the entoconid and the acquisition of a soricine-like p4, supports a strong relationship between *Paenelimnoecus* and *Allosorex*, anchoring the genus into the Allosoricinae.

Subfamily Soricinae Fischer, 1814
Tribe Soricini Fischer, 1814
Genus *Paenesorex* Ziegler, 2003

Type species.—*Paenesorex bicuspis* Ziegler, 2003, by monotypy.

Occurrence.—MN7/8 of Germany (Ziegler, 2003; Prieto, 2007) and Hungary (Hír et al., 2016) and MN9 of Slovakia (this paper).

Paenesorex bicuspis Ziegler, 2003, and
Paenesorex cf. *P. bicuspis* Ziegler, 2003
Figures 3.7–3.15, 5.1

Holotype.—Left mandible with i1–m3, NHMA P6-01051 A1, Petersbuch 6, Germany (Ziegler, 2003).

Description.—The dental pigmentation is moderate, reaching the base of most cusps and cuspids.

Several fragments of maxillary are preserved. One of them shows three complete alveoli anterior to the P4 (Fig. 3.8). The posteriormost alveolus is circular and is interpreted as belonging to the A4. The anteriormost complete alveolus is elongated and interpreted as belonging to the A2. Anterior to it, a partly preserved larger alveolus is present, which is interpreted as belonging to the A1. The infraorbital foramen is enlarged. It starts slightly anterior to the posterolabial root of the P4 and ends above the mesostyle of the M1. A small lacrimal aperture is found directly above the posterior root of the M1.

The I1 is compact, with a strongly curved anterodorsal margin. The talon is thick and bears a pointy cuspule. The lingual cingulum creates an angular posterodorsal corner in labial view. The A2 is a relatively short, quadrangular element bearing a laterally compressed cusp in anterior position. A central crest is present, reaching the oblique postcrista. The antemolar is exaenodont. The lingual cingulum is also stronger. The P4 is a gracile element with a high paracone and a short, sharp postparacrista. The low parastyle is pointy and connected to the base of the paracone. A low, straight ridge connects the parastyle to the small protocone. The hypocone is included in a curved crest weakly connected to the protocone. The posthypocrista continues until the posteriormost part of the lingual region and joins the posterior cingulum. The posterior emargination is deep.

The M1 shows the classic soricine morphology. On the W-shaped labial crest complex, the parastyle creates a small hook on unworn specimens. The preprotocrista is slightly curved. Rarely, a thin and low crest connects the postprotocrista to the base of the metacone (metaloph). The hypocone is low and included in a ridge running along the posterior flank. The M2 differs from the M1 only by the slightly smaller dimensions and the more reduced posterolingual area (Fig. 3.10). The M3 is a moderately compressed, subtriangular molar with an elongated preparacrista and a short, slightly curved postparacrista. The metacone is included in the premetacrista. The mesostyle area is not divided. The protocone is very low. A thin posthypocrista is present, closing the broad basin without joining the metacone.

The i1 is bicuspulate, has a weak posterolabial cingulid and a narrow root (Fig. 3.11).

The m1 has a narrow trigonid with a relatively high paraconid bearing a short anterior swelling. The paralophid shows a deep carnassial notch. The metaconid is higher than the paraconid. The hypoconid is connected to the trigonid wall by a bi-partitioned oblique cristid. This crest is superficially divided by a moderate carnassial notch (Fig. 3.12). The hypolophid is straight. The entoconid is strong and the entocristid moderately high. The postentoconid valley is broad. The molar is surrounded by a narrow cingulid. The m2 differs from the m1 by the broader trigonid and slightly weaker notch on the paralophid and oblique cristid. The m3 has a trigonid with a high paraconid showing a short anterior swelling. The paralophid is bi-partitioned. The metaconid is as high as the paraconid. The talonid is characterized by a continuous U-shaped cristid. On unworn specimens, the hypoconid is barely distinguishable. Broad labial and anterior cingula are present.

Material.—See Table 2 for measurements. Borský Svätý Jur (*P. bicuspis*): eight I1, one A2, two fragments of maxillary with P4–M1, three P4, one fragment of maxillary with M1, one fragment of maxillary with M1–M2, ten M1, 22 M2, six i1, one fragment of mandible with m1–m3, one fragment of mandible with m1–m2, two fragments of mandibles with m1, eight m1, two fragments of mandibles with m2–m3, six m2, one mandible with m3, two m3.

Studienka A (*P. bicuspis*): one M1, two M2, one M3, two i1, three m1, one fragment of mandible with m2–m3, one fragment of mandible with m2, five m2, one m3.

Studienka D (*P.* cf. *P. bicuspis*): one M2 (BL = 1.22, PE = 0.97, LL = 1.16, AW = 1.55, PW = 1.47).

Remarks.—The species from Borský Svätý Jur and Studienka (A and D) is an unspecialized Soricini showing most of the features of *Paenesorex bicuspis*. Namely, the lacrimal foramen above the posterior root of the M1, the four single-rooted teeth between the upper incisor and the P4, the moderate to strong posterior emargination on P4-M1, the bicuspulate i1, the m1 and m2 with low entocristid and broad postentoconid area and the m3 with a reduced talonid displaying a low hypoconid.

The few differences that have been found with the type material described by Ziegler (2003) are (1) the slightly smaller size, (2) the slightly deeper posterior emargination of the P4, (3) the presence of a small carnassial notch in the oblique cristid of the most unworn m1, and (4) the somewhat lower hypoconid on m3. It is unclear whether these differences are actually found in the variability of the material from Petersbuch 6 or if they indicate a slight temporal shift in the morphological and morphometrical variability of the species.

https://doi.org/10.1017/jpa.2024.23 Published online by Cambridge University Press

Table 2. Measurements (in mm) of *Paenesorex bicuspis* from Borský Svätý Jur (MN9) and Studienka A (MN9), Slovakia. AW = anterior width; BL = labial length; H = height; L = length; LL = lingual length; LT = length of the talon; N = number of specimens; PE = length of the posterior emargination; PW = posterior width; TAW = talonid width; TRW = trigonid width; W = width.

Paenesorex bicuspis, Borský Svätý Jur																	
	I1			P4				M1					M2				
	L	LT	H	BL	PE	LL	W	BL	PE	LL	AW	PW	BL	PE	LL	AW	PW
N	8	8	8	5	3	3	3	9	10	11	9	7	16	13	9	12	8
Min	1.21	0.57	0.85	1.25	0.57	0.73	1.20	1.25	0.90	1.20	1.33	1.40	1.12	0.85	1.09	1.29	1.34
Max	1.31	0.70	0.95	1.49	0.65	0.91	1.28	1.37	1.03	1.37	1.48	1.70	1.29	1.10	1.31	1.47	1.54
Mean	1.26	0.63	0.90	1.36	0.62	0.83	1.25	1.31	0.97	1.29	1.39	1.54	1.21	0.94	1.18	1.41	1.41
	i1		m1			m2			m3								
	L	H	L	TRW	TAW	L	TRW	TAW	L	W							
N	1	2	8	9	9	10	10	10	5	5							
Min	—	0.73	1.21	0.66	0.72	1.16	0.66	0.68	0.91	0.53							
Max	—	0.77	1.35	0.72	0.79	1.26	0.76	0.78	0.95	0.59							
Mean	2.62	0.75	1.26	0.70	0.75	1.20	0.71	0.73	0.93	0.56							
Paenesorex bicuspis, Studienka A																	
	P4	M1		M2				M3		m1			m2			m3	
	BL	BL	PE	BL	PE	LL	PW	L	W	L	TRW	TAW	L	TRW	TAW	L	W
N	1	1	1	1	1	1	1	1	1	1	1	3	5	5	6	2	2
Min	—	—	—	—	—	—	—	—	—	—	—	0.78	1.20	0.74	0.76	0.96	0.59
Max	—	—	—	—	—	—	—	—	—	—	—	0.82	1.31	0.79	0.81	0.97	0.61
Mean	1.34	1.33	1.03	1.28	1.01	1.05	1.27	0.66	1.17	1.32	0.73	0.80	1.25	0.77	0.79	0.97	0.60

Genus *Isterlestes* new genus

Type species.—*Isterlestes aenigmaticus* n. sp., by monotypy.

Diagnosis.—as for type species by monotypy.

Etymology.—From ister (Ἴστρος), the ancient Greek name of the Danube; and lestes (λῃστής), thief, bandit, a commonly used suffix for insectivore genera.

Remarks.—The combination of pigmented teeth, fissident I1, unspecialized P4, P4–M2 with moderate to strong posterior emargination, tricuspulate i1, and lower molars with broad talonid and developed entocristid undoubtedly anchors *Isterlestes* n. gen. within the Soricini. See remarks for *Isterlestes aenigmaticus* n. gen. n. sp. for additional discussion.

Isterlestes aenigmaticus new species
Figures 4, 5.3

Holotype.—SG198641; Šalgovce 5, Slovakia; right fragment of maxillary with A4 (L = 0.23, W = 0.33), P4 (BL = 1.08, PE = 0.70, LL = 0.78, W = 1.13), M1 (BL = 1.15, PE = 0.86, LL = 1.11, AW = 1.20, PW = 1.26), and M2 (BL = 1.07, PE = 0.86, LL = 1.03, AW = 1.25, PW = 1.20) (Figs. 4.3, 5.3).

Paratypes.—SG198615–SG198640 (26 specimens): four I1, one P4, two M1, eight i1, five m1, one fragment of mandible with m2, two m2, three m3. The extractable dental measurements are provided in Table 3.

Diagnosis.—Differing from other soricinine species by the following combination of characters: small size (Lm1 ≃ 1.20); large infraorbital foramen above M1; small lacrimal aperture above the anterior root of the M2; weak to moderate dental pigmentation; fissident I1; extremely reduced A5; compressed A4; P4 with low parastyle, low protocone, and rounded lingual margin; M1 and M2 with a crest connecting the postparacrista to the base of the metacone and a low hypocone; P4–M2 with a moderate to strong posterior emargination; tricuspulate i1; m1–m2 with distinct entocristid and entoconid; reduced m2 (Lm1/Lm2 ≃ 1.25).

Differential diagnosis.—Differs from all Neogene Soricini by the posterior displacement of the infraorbital foramen and the lacrimal aperture (Fig. 5.3), and by reduction of the A5 and the m2. Additionally, differs from *Deinsdorfia* by the fissident I1, shorter P4, unreduced M2, and significantly lower structures on upper molars; from *Dimylosorex* by the unspecialized dentition (unreduced number of antemolar, simple P4, presence of m3). Differs from *Paenesorex* by the reduced A4, the more compact P4, the broader M1–2, the lower dental structure on upper and lower molars, and the tricuspulate i1. Differs from most *Sorex* by the fissident I1. Differs from all *Sorex* by the reduction of the A4 and the lower cusps on P4. Differs from *Zelceina* by the fissident I1, stronger posterior emargination on P4–M2, and (except *Z. kormosi* Storch, 1995) the tricuspulate i1.

Occurrence.—Šalgovce 5, Topoľčany district, Nitra Region (Slovakia), Danube basin. Correlated to middle Turolian, MN12.

Description.—The dental elements show a weak to moderate dental pigmentation.

The infraorbital foramen is large (0.90 mm; 78% of M1 labial length). It starts above the P4/M1 and ends above the posterolabial root of the M1. Viewed from above, the infraorbital foramen is broad, as the maxillary is strongly curved. Namely, the rostral height appears short. The small lacrimal aperture is found above the anterior root of the M2. The anteriormost part of the orbit is found above the middle part of the M2 (directly above the mesostyle). This leads to a short breadth of the bony bridge (0.77 mm; 67% of M1 labial length). In occlusal view, a very small and rounded alveolus is found between the A4 and the P4 (Fig. 4.3). This alveolus is situated

https://doi.org/10.1017/jpa.2024.23 Published online by Cambridge University Press

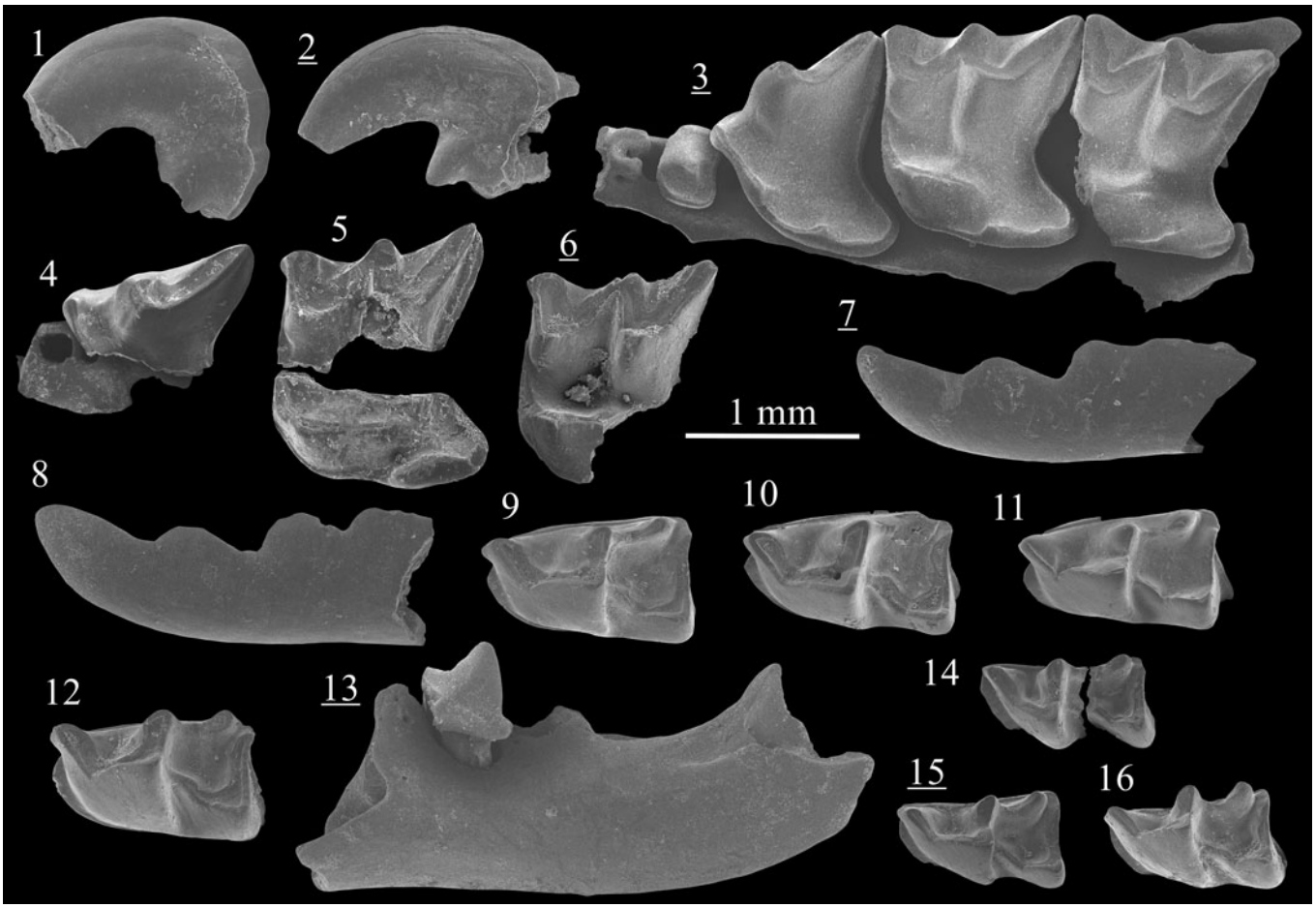

Figure 4. Scanning electron photomicrographs of *Isterlestes aenigmaticus* n. gen. n. sp. from Šalgovce 5. (**1**) (paratype) I1, SG198634, labial view; (**2**) (paratype) I1, SG198635, labial view; (**3**) (holotype) fragment of skull with A4, P4–M2, SG198641; (**4**) (paratype) P4, SG198638; (**5**) (paratype) M1, SG198639; (**6**) (paratype) M1, SG198640; (**7**) (paratype) i1, SG198616, labial view; (**8**) (paratype) i1, SG198617, labial view; (**9**) (paratype) m1, SG198623; (**10**) (paratype) m1, SG198624; (**11**) (paratype) m1, SG198626; (**12**) (paratype) m1, SG198618; (**13**) (paratype) fragment of mandible with m2, SG198630; (**14**) (paratype) m2, SG198631; (**15**) (paratype) m2, SG198632; (**16**) (paratype) m2, SG198633. Images with underlined numbers are reversed.

slightly lingually, so that the parastyle of the P4 and the posterolabial lobe of the A4 occupy all the labial margin of the maxillary (Fig. 5.3). Anterior to the compressed A4, a more elongated alveolus is found, with an elevated anteriormost part. Above this alveolus (A3) is found a tiny supra infraorbital foramen.

The I1 is slightly fissident and has a strongly curved dorsal margin. The posterior talon has a slightly projected labial cuspule and a posterolingual thickening. In labial view, the cingulum extends all along the posterior margin and reaches the center of the dorsal margin.

The A4 is a small, anteroposteriorly compressed antemolar with a minute cusp in anterior position and two symmetrical lobes. A thin and central ridge connects the cusp to the posterior margin. A continuous cingulum, weaker on the anterior flank, surrounds the tooth. The P4 bears a high paracone and short postparacrista. All other structures are extremely low (Fig. 4.3). The parastyle is connected to the base of the paracone by a thin ridge and is slightly eccentric in occlusal view. The parastyle is connected by a straight ridge to a barely distinct protocone. A curved prehypocrista is present. The low hypocone is in a more posterior position than the paracone. The posthypocrista joins the posterior cingulum. The posterior emargination is moderately deep (PE index = 0.33).

The M1 has a high labial complex with relatively short preparacrista and premetacrista. The parastyle creates a small hook at the anterolabial corner. The protocone is low and elongated. The preprotocrista is curved. A thin postprotocrista descends from the protocone and ends freely in the middle of the lingual area. A thin crest connects the middle section of the postprotocrista to the base of the metacone. The hypocone is low and connected to the posterior cingulum by a marked posthypocrista. The posterior emargination is moderate (PE index = 0.31). The M2 differs from the M1 by the longer preprotocrista, the shorter postmetacrista, the stronger connection between the postprotocrista and the base of the metacone, the slightly reduced posterolingual extension, and the shallower posterior emargination (PE index = 0.22).

Only a fragment of a mandible is known. It displays a very thin ramus, a fragment of m2, and the two alveoli of the m3 (Fig. 4.13). The posterior alveolus is more elongated than the anterior one. The maximal length of the m3 alveoli is 0.87 mm.

The i1 is always tricuspulate. The posteriormost cuspule is weakly (Fig. 4.7) to strongly (Fig. 4.8) developed. The apex is

https://doi.org/10.1017/jpa.2024.23 Published online by Cambridge University Press

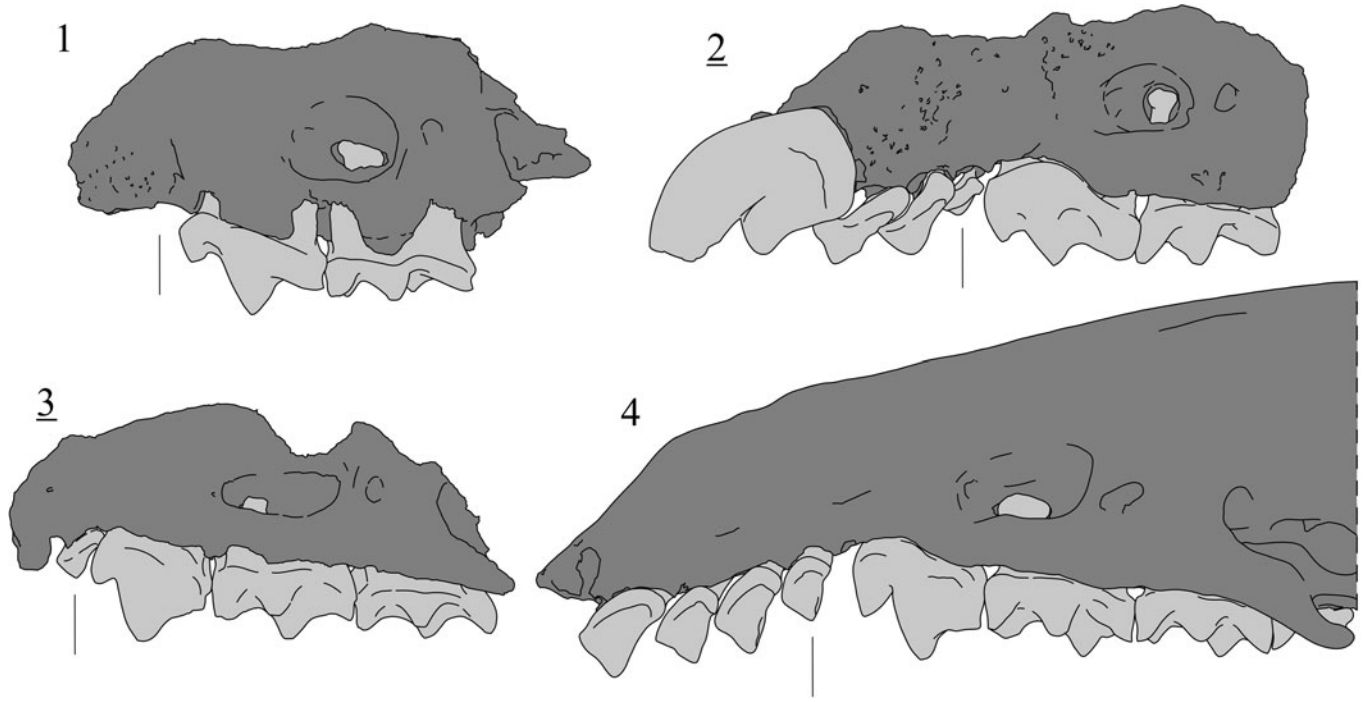

Figure 5. Comparative drawing of the cranial structures of several Soricini genera (unscaled), in labial view. Black lines indicate the position of the A4. (**1**) *Paenesorex bicuspis*, Borský Svätý Jur (MN9), Slovakia, BJ213719; (**2**) *Zelceina soriculoides* (Sulimski, 1959), Węże 1 (MN14), Poland, MF/1859/4; (**3**) *Isterlestes aenigmaticus* n. gen. n. sp., Šalgovce 5 (MN12), Slovakia, SG198641 (holotype); (**4**) *Sorex minutus*, Charente (Recent), France, RC000001. Images with underlined numbers are reversed.

slightly bent upward. A continuous and narrow inner cingulid is present.

The m1 has a triangular trigonid and broad talonid. The paraconid is pointy and slightly bent. The paralophid consists of two straight crests superficially divided by a moderate carnassial notch. The metalophid is bi-partitioned and the metaconid is higher than the paraconid. The entoconid is high and laterally compressed. The entocristid is low. The hypoconid is slightly lower than the entoconid and is connected to the trigonid wall by a bi-partitioned oblique cristid. The hypolophid is low and the postentoconid valley is distinct. Narrow anterolabial, posterior and lingual cingulids are present. The anterior cingulid is broader but lacking below the paraconid. The m2 is a small version of the m1, with a narrow, triangular trigonid and broad talonid. The metaconid is only slightly higher than the paraconid. The oblique cristid is low and bi-partitioned. The hypolophid reaches the lingual margin, leading to a narrow postentoconid valley. The anterior cingulid is broad. The lingual and posterior cingulid are continuous but very narrow.

Etymology.—From the Latin aenigmaticus, a, um: enigmatic, puzzling. In reference to its obscure relationship with other Soricini, and especially with early *Sorex*-like species.

Remarks.—As stated by Ziegler (2003), *Paenesorex* does not constitute a convincing structural ancestor for *Sorex*. This is also true for *Isterlestes* n. gen. The combination of bicuspulate i1 indicates that *Paenesorex* displays a more ancestral morphological grade and has a sharper dentition that is better suited for the consumption of soft-bodied organisms. *Paenesorex* displays a broad and circular infraorbital foramen in labial view (Fig. 5.1). This is a consequence of a rather

Table 3. Measurements (in mm) of *Isterlestes aenigmaticus* n. gen. n. sp. from Šalgovce 5 (MN12), Slovakia. AW = anterior width; BL = labial length; H = height; L = length; LL = lingual length; LT = length of the talon; N = number of specimens; PE = length of the posterior emargination; PW = posterior width; TAW = talonid width; TRW = trigonid width; W = width.

	I1			A4		P4				M1				
	L	LT	H	L	W	BL	PE	LL	W	BL	PE	LL	AW	PW
N	1	2	2	1	1	2	1	1	1	3	1	2	1	1
Min	—	0.71	1.11	—	—	1.08	—	—	—	1.08	—	1.11	—	—
Max	—	0.75	1.16	—	—	1.19	—	—	—	1.15	—	1.14	—	—
Mean	1.50	0.73	1.13	0.23	0.33	1.13	0.70	0.78	1.13	1.12	0.86	1.13	1.20	1.26
	M2					i1	m1			m2				
	BL	PE	LL	AW	PW	H	L	TRW	TAW	L	TRW	TAW		
N	1	1	1	1	1	4	4	5	7	3	3	4		
Min	—	—	—	—	—	0.71	1.18	0.64	0.70	0.93	0.51	0.53		
Max	—	—	—	—	—	0.84	1.22	0.66	0.77	0.99	0.51	0.65		
Mean	1.07	0.86	1.03	1.25	1.20	0.78	1.20	0.65	0.73	0.96	0.51	0.58		

https://doi.org/10.1017/jpa.2024.23 Published online by Cambridge University Press

straight maxillary face and a high rostral height, as indicated by a well-preserved skull from Petersbuch 6 (P6-01053A1; Ziegler, 2003: fig. 5.3). Consequently, *Paenesorex* likely occupied a basal position within the Soricini.

Overall, a significant number of the diagnostic features of *Isterlestes aenigmaticus* n. gen. n. sp. indicates a slight shortening of the face, which is unusual for Soricini. This snout shortening is accompanied by lowering of the crests and cusps on the upper dentition. This supports a change in the dietary preferences of the species, in which the P4 and the molars became of higher importance for masticatory purposes. This slight dietary specialization is not equivalent to the extremely robust dentition of *Zelceina*, which displays massive antemolars, elongated P4, and A5 still visible in labial view (Fig. 5.2). Similarly, *Deinsdorfia* is also extremely specialized (Furió and Mein, 2008). Its first probable occurrence, in the MN7/8 of Petersbuch 31 (Ziegler, 2003), indicates a very early morphological diversification of the Soricini. *Zelceina* is identified slightly later, from MN11 onwards (Rzebik-Kowalska and Nesin, 2010; Rzebik-Kowalska and Rekovets, 2016). Notably, both *Zelceina* and *Deinsdorfia* possess the peculiar *Blarina*-type schmelzmuster structure (von Koenigswald and Reumer, 2020), which is not present in *Sorex*. We consider here *Paenesorex* as a true Soricini, *Zelceina* and *Deinsdorfia* likely acquired this structure independently from the Blarinini, which strongly indicates that these two genera belong to a subgroup of specialized Soricini that is different from *Sorex* and *Isterlestes* n. gen.

Most of our knowledge on the oldest European *Sorex* are based on karst deposits from the Ruscinian of central Europe (e.g., Sulimski, 1962; Reumer, 1984). This is in line with molecular data (e.g., Bannikova et al., 2018), supporting that the early history of *Sorex* is missing in the fossil record. This extends to the Soricini and is likely a consequence of poor preservation and overall rare presence of this tribe in the Middle and Late Miocene of Eurasia. It also appears that delimitation of the genus *Sorex* is still blurry (Reumer, 1984). However, the posterior displacement of the infraorbital foramen and lacrimal aperture and the reduction of the A4, the A5 (Fig. 5.3), and the m2 in the species from Šalgovce 5 support a separate generic assignment. Such features imply that *Isterlestes aenigmaticus* n. gen. n. sp. does not constitute a good structural ancestor for any Neogene Eurasian species of *Sorex* (e.g., *S. bor* Reumer, 1984, *S. ertemteensis* Storch, 1995, *S. hibbardi* Sulimski, 1962, *S. minutus* Linnaeus, 1766, *S. minutoides* Von Zimmermann, 1780, *S. polonicus* Rzebik-Kowalski, 1991, *S. prealpinus* Heller, 1930, *S. pseudoalpinus* Rzebik-Kowalski, 1991, *S. runtonensis* Hinton, 1911, *S. subminutus* Sulimski, 1962) or for any recent species having deep roots within the phylogeny of *Sorex* (e.g., *S. alpinus* Schinz, 1837, *S. cinereus* Kerr, 1792). However, few permutations are necessary to pass from a *Sorex*-like dental structure to *Isterlestes* n. gen. Additionally, both *Sorex* and *Isterlestes* show an elongated infraorbital foramen (Fig. 5), although *Isterlestes* likely has a shorter rostral height.

Considering the lack of important dentognathic elements (p4, m3, mandibular condyles), it is unclear how close *Isterlestes aenigmaticus* n. gen. n. sp. and *Sorex* are, from a phylogenetic perspective. The dental and cranial structures described here suggest that *Isterlestes* diverged before the appearance of *Sorex*. However, this is partly contradicted by the estimated age of emergence of *Sorex* around the late Early Miocene (Bannikova et al., 2018), but the calibration (Bannikova et al., 2018, table S3) leading to this likely overestimated age is actually based on scant Late Miocene evidence from Asia and North America (Bown, 1980; Storch and Qiu, 1991). Because *Sorex* was probably not yet present in Europe before MN13 (based on Doukas et al., 1995), there is no taxonomic or biogeographic evidence supporting that *Isterlestes* n. gen. emerged from an early *Sorex*. This strengthens even more the role of central Europe in the evolution and morphological experimentation of the Soricini.

Tribe Anourosoricini Anderson, 1879

Genus *Crusafontina* Gibert, 1975

Type species.—*Crusafontina endemica* Gibert, 1975.

Other referred species.—*Crusafontina kormosi* (Bachmayer and Wilson, 1970); *C. exculta* (Mayr and Fahlbusch, 1975); *C. magna* Hutchison and Bown in Bown, 1980); *C. minima* Hutchison and Bown in Bown, 1980; *C. fastigata* Van Dam, 2004; *C. vandeweerdi* Van Dam, 2004.

Diagnosis.—See Van Dam (2004, p. 743).

Occurrence.—*Crusafontina* is a widespread genus identified in the late Middle Miocene and Late Miocene of Europe (Mészáros, 1998a; Van Dam, 2004; Ziegler, 2006b), Turolian of Asia (Zazhigin and Voyta, 2022) and early Late Miocene of North America (Bown, 1980; Van Dam, 2010). Ziegler (2006a) included *C. exculta* in *C.* aff. *C. endemica*, which is not followed here because Van Dam (2010) clearly demonstrated the peculiarities of the species from Hammerschmiede.

Crusafontina endemica Gibert, 1975

Figure 6

Holotype.—Fragment of left mandible with p4–m2, ICP nr. 9009, Can Llobateres, Spain (Gibert, 1975).

Diagnosis.—See Van Dam (2004, p. 744).

Occurrence.—From MN9 and MN10 of Europe (Gibert, 1975; Mészáros, 1998a, 1999; Van Dam, 2004; Ziegler, 2006a, b; Rzebik-Kowalska and Lungu, 2009).

Description.—The I1 is a massive incisor with an evenly rounded labial outline in lateral view. The apex tip is sharp, slightly procumbent and bent mesially. The talon is low and rounded in lateral view. A distinct notch is present between the talon and the apex tip (Fig. 6.1). The labial cingulum is present below the talon. The A1 has a laterally compressed main cusp, a thick anterior crest reaching the pointy anterior margin and a thinner posterior one joining the posterior cingulum. The antemolar is exaenodont and the lingual flank bears a minute cusp on the center of the thick cingulum (Fig. 6.2). The posterolingual part bears a shallow basin delimited by a robust cingulum. The A2 is distinct from the A1 by being less elongated and by having no minute cusp on

https://doi.org/10.1017/jpa.2024.23 Published online by Cambridge University Press

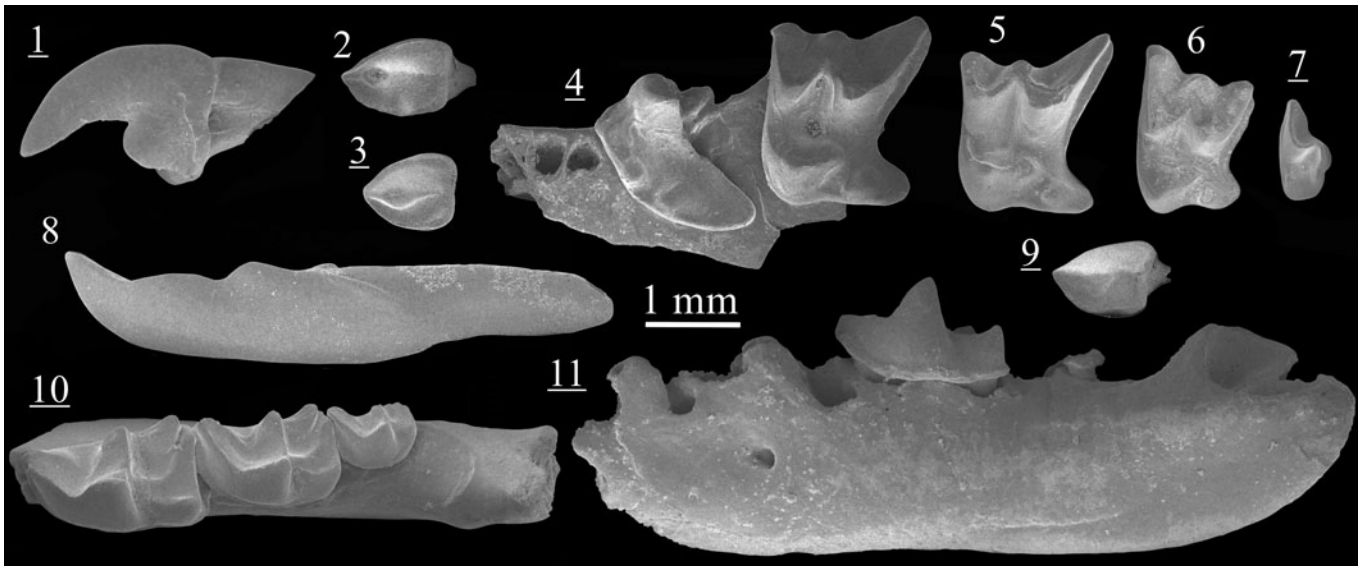

Figure 6. Scanning electron photomicrographs of *Crusafontina endemica* from Borský Svätý Jur (**1–10**) and Studienka A (**11**). (**1**) I1, BJ213600, labial view; (**2**) A1, BJ213607; (**3**) A2, BJ213672; (**4**) fragment of maxillary with P4–M1, BJ213612; (**5**) M1, BJ213616; (**6**) M2, BJ213628; (**7**) M3, BJ213633; (**8**) i1, BJ213642, labial view; (**9**) a1, BJ213682; (**10**) fragment of mandible with m2, BJ213652, labial view; (**11**) fragment of mandible with m1–m3, ST214364. Images with underlined numbers are reversed.

the lingual cingulum. The posterolingual corner is elevated. The P4 has a conical paracone and a thick, slightly curved postparacrista. A thin preparacrista is present between the paracone and the parastyle. A thin crest extends from the parastyle and reaches the slightly lower protocone. The hypocone is lower and situated more posteriorly than the protocone. The hypoconal flange is stretched and surrounded by a cingulum. The posterior emargination is moderately deep.

The M1 has a strong metacone. The premetacrista is slightly higher than the postparacrista. The preparacrista is short and turns as a hook when joining the parastyle at the anterolingual corner. The postmetacrista is sharp, long and slightly curved. From the protocone extends a preprotocrista not connected to the paracone. The end of the postprotocrista is thickened. On the most posterolabial part of the postprotocrista are found: no crests (five, all from BJ; Fig. 6.4, 6.5), a short freely ending crest (one in BJ, two in ST A), or a crest joining the lingual base of the metacone (one in ST A). The hypocone is low and independent from the postprotocrista. It has an elongated hypoconal flange. There is a broad cingulum along the base of the postmetacrista. On M2, the metacone is still stronger than the paracone. The preparacrista is slightly longer than the postparacrista, premetacrista and postmetacrista. The postprotocrista is thicker posteriorly. The hypocone is low and less extended than in M1. The hypoconal flange is less stretched than in M1 (Fig. 6.5 vs. Fig. 6.6). The M3 is strongly reduced. The paracone is the highest cusp and leads to a curved preparacrista and a short postparacrista. The metacone is indistinct from the curved premetacrista, which is connected by a straight descending crest to a barely visible hypocone. A short preprotocrista is present.

The body of the mandible is regular in height. The upper part of the angular process ends at three quarters the height of the body. The mandibular foramen is located below the anterior root (in one case), between the two roots (in two cases; Fig. 6.11) or almost below the posterior root of the m1 (in one case).

The lower incisor is bicuspulate (Fig. 6.8). The tip of the cusp is bent upward and slightly mesially. There is a continuous and curved cingulum on the mesial side. On the labial side, the posterior cingulum is barely visible. The a1 is subtriangular, relatively flat and exaenodont. The main cusp is laterally compressed. It is connected to the anterior margin by a robust crest. A much thinner posterior crest connects the cusp to the straight posterior margin. A continuous cingulid is present, thicker at the posterolingual and posterolabial corner. The p4 is subtriangular and exaenodont. The main cuspid is slightly laterally compressed and relatively high. From this cuspid extends a thick and curved crest reaching the anterior margin. A thinner crest reaches the slightly oblique posterior border.

The trigonid of m1 is longer than the talonid. The paralophid is bi-partitioned. The metaconid is higher than the paraconid. The trigonid basin is largely open lingually. The trigonid displays two morphotypes: the morphotype A (sensu Furió, 2007, fig. 6.13) has clearly separated protoconid and metaconid (three in BJ; two in ST A; Fig. 6.10), whereas the morphotype B displays an anteriorly elongated trigonid with close protoconid and metaconid (two in BJ; one in ST A). The hypoconid is larger and lower than the entoconid. The oblique cristid is almost parallel to the tooth anteroposterior axis, connecting just lingually to the base of the protoconid. The entocristid touches the base of the metaconid. The entostylid is strongly separated from the entoconid. The postentoconid valley is narrow. Short and narrow cingula are present anteriorly, labially and posteriorly. The m2 differs from the m1 by the smaller size, the narrower talonid and the lack of trigonid displaying the morphotype B. The trigonid of the m3 is only slightly reduced (Fig. 6.10). The paraconid and the metaconid have the same height. The anteriormost part of the paralophid is slightly curved. The talonid is moderately reduced, with a shallow basin completely closed by a continuous U-shape crest. In one of the two unworn specimens from BJ, a small entoconid

https://doi.org/10.1017/jpa.2024.23 Published online by Cambridge University Press

Table 4. Measurements (in mm) of *Crusafontina endemica* from Borský Svätý Jur (MN9) and Studienka A (MN9), Slovakia. AW = anterior width; BL = labial length; H = height; L = length; LL = lingual length; LT = length of the talon; N = number of specimens; PE = length of the posterior emargination; PW = posterior width; TAW = talonid width; TRW = trigonid width; W = width.

Crusafontina endemica, Borský Svätý Jur															
	I1			A1		A2		P4			M1				
	L	LT	H	L	W	L	W	PE	LL	W	BL	PE	LL	AW	PW
N	3	3	4	4	5	3	4	2	2	2	6	7	6	4	4
Min	2.12	0.99	1.45	1.41	0.92	0.99	0.79	1.19	1.38	1.76	1.70	1.23	1.53	1.77	1.96
Max	2.21	1.07	1.57	1.51	1.00	1.09	0.84	1.20	1.45	1.80	1.84	1.38	1.74	2.01	2.18
Mean	2.16	1.02	1.51	1.45	0.96	1.04	0.81	1.19	1.42	1.78	1.77	1.33	1.62	1.88	2.05
	M2					M3		i1		a1		p4			
	BL	PE	LL	AW	PW	L	W	L	H	L	W	L	W		
N	2	4	2	3	2	2	2	3	3	3	2	2	2		
Min	1.30	1.06	1.19	1.87	1.41	0.60	1.14	3.84	1.10	0.96	0.78	1.26	0.87		
Max	1.31	1.09	1.24	1.94	1.52	0.66	1.17	4.07	1.17	1.04	0.87	1.32	0.90		
Mean	1.30	1.08	1.21	1.91	1.46	0.63	1.16	3.94	1.13	1.00	0.83	1.29	0.98		
	m1			m2			m3								
	L	TRW	TAW	L	TRW	TAW	L	TRW	TAW						
N	3	4	2	2	3	3	3	4	2						
Min	1.66	0.97	1.16	1.65	0.96	0.92	1.06	0.63	0.51						
Max	1.90	1.09	1.19	1.66	1.04	1.06	1.17	0.71	0.62						
Mean	1.79	1.05	1.17	1.65	0.99	1.00	1.12	0.67	0.56						
Crusafontina endemica, Studienka A															
	I1		P4				M1					m1			
	L	H	L	PE	LL	W	BL	PE	LL	AW	PW	L	TRW	TAW	
N	1	2	1	1	1	1	1	1	1	2	1	1	2	2	
Min	—	1.65	—	—	—	—	—	—	—	2.03	—	—	1.03	1.10	
Max	—	1.65	—	—	—	—	—	—	—	2.08	—	—	1.06	1.15	
Mean	2.48	1.65	1.70	1.29	1.50	2.07	1.84	1.26	1.50	2.06	2.03	1.94	1.04	1.12	
	m2			m3											
	L	TRW	TAW	L	TRW	TAW									
N	1	1	2	1	1	1									
Min	—	—	0.90	—	—	—									
Max	—	—	0.98	—	—	—									
Mean	1.60	1.02	0.94	0.96	0.66	0.61									

and hypoconid are found at the posterolingual and posterolabial corners, respectively.

Material.—See Table 4 for measurements. Borský Svätý Jur: five I1, five A1, four A2, one fragment of maxillary with P4-M1, two P4, nine M1, six M2, two M3, six i1, three a1, two p4, one fragment of mandible with m1, five m1, one fragment of mandible with m2, four m2, four m3.

Studienka A: three I1, one P4, two M1, one M2, three i1, one fragment of mandible with m1–m3, three m1, two m2.

Remarks.—The combination of moderate size, lack of parastyle on A1, wide M1 with posterior emargination, elongated trigonid on m1, entocristid on m1 and m2, straight oblique cristid, and a relatively small M2 and m3 with still a functional talon are clear indicators of *Crusafontina*. Several Late Miocene lineages of *Crusafontina* have been identified (Van Dam, 2010), but central Europe, an apparent source area for Late Miocene Anourosoricini (Van Dam, 2004; this paper), was mostly occupied by the main *C. endemica*–*C. kormosi* lineage (e.g., Ziegler, 2006a, b). Our MN9 material displays strong similarities with *Crusafontina endemica*, based on the relatively small size, the gracile A1, the bicuspulate i1, and the slightly reduced m3. The material from our oldest locality, Borský Svätý Jur, already displays all the diagnostic features differentiating *C. endemica* from *C. exculta* (see Van Dam, 2010). The Lm3/Lm1 ratio equals 0.61 in Borský Svätý Jur and 0.50 in Studienka A, which are typical values for *C. endemica* (based on Van Dam, 2004; Ziegler, 2005, 2006a).

Several Vallesian *Crusafontina* from central European have been attributed to *C.* aff. *C. endemica* (see Ziegler, 2005, 2006a) because of a mental foramen in a more posterior position and overall, a deeper ectoflexus on M1. In addition, the m3 from Rudabánya displays a two-cusped talonid (Ziegler, 2005), whereas the talonid in the type material of Can Llobateres is apparently more reduced.

In our four fragments, BJ213652 has a mental foramen at the same position as specimen CL1 2256 from Can Llobateres (Van Dam, 2004, fig. 3.3), whereas BJ213654 is very similar to NHMW-272 from Rudabánya (Ziegler, 2005, pl. 4.1). Thus, the position of the mental foramen is affected by variation, including its presence below the anterior alveolus of the m1. The depth of the ectoflexus on M1 differs between species, but also shows a gradual evolution within lineages. It is not surprising that the MN10 and the comparatively fewer late MN9 materials from Austria are more advanced than the peripheral occurrences from MN9 of Spain. Such gradual evolution is also apparent in the Austrian, Hungarian, and Slovak material. Similarly, the development of m3 is subject to gradual intraspecific change. The type material of *C. endemica*, from Can Llobateres, still preserves the entoconid and the hypoconid (Gibert, 1975). However, in his description of *C. endemica* from MN9 in Spain, Van Dam (2004) figured a m3 with distinct cuspids (fig. 2.21) from this locality, alongside another m3 with only a continuous talonid cristid from Puente Minero 2 (Van Dam, 2004, fig. 2.13). The material from Borský Svätý Jur has one specimen out of two showing distinguishable talonid cuspids. Ziegler (2006a) considered that the poorly reduced m3 in the material from

https://doi.org/10.1017/jpa.2024.23 Published online by Cambridge University Press

Rudabánya discard was an attribution to *C. endemica*, but this is based on only two specimens. Likely, the distinction of these cuspids is correlated to a high Lm3/Lm1 ratio, explaining the higher frequency of these features in apparently older material.

The validity of *Crusafontina* aff. *C. endemica* in central Europe is based on morphological particularities that are all explainable by morphological variability and slight gradual changes. Here, we reclassify the material from Rudabánya, Götzendorf, Richardhof–Golfplatz, Richardhof–Wald, and Schernham as *Crusafontina endemica*. The limited sample from Neusiedl am see is reclassified as *Crusafontina* cf. *C. endemica*.

Crusafontina kormosi (Bachmayer and Wilson, 1970)
Figure 7

Holotype.—Fragment of right mandible with m1–3, NHMW 1970/1389, Kohfidisch, Austria (Bachmayer and Wilson, 1970).

Diagnosis.—See Van Dam (2004, p. 750).

Occurrence.—MN10 and MN11 of Europe (Van Dam, 2004; Ziegler, 2006a, b; Ménouret and Mein, 2008). *Crusafontina kormosi* is also recorded in MN12 and earliest MN13 of Hungary (Mészáros, 1998a, b, 1999) and suspected in MN13 of Moldova (Rzebik-Kowalska and Lungu, 2009).

Description.—An almost complete maxillary is preserved, with all elements except A3 and M3 (Fig. 7.11). Between the A2 and the P4, a small, circular alveolus is found. The available space implies a relatively ovoid A3. A tiny foramen is present above the root of the A2. The entrance of the infraorbital fossa is situated above the posterolabial root of the P4.

The I1 is a massive tooth with a sharp and projected tip (Fig. 7.10). The labial cingulum is thicker in its median part. The A1 is a strongly elongated tooth with a laterally compressed cusp and robust centrocrista (Fig. 7.1, 7.11). The posterolingual area displays a talon with a minute cusp and a second, less distinct bulge in a more central position. A posterior emargination is present, separating the lingual complex from the simple labial flank. Cingulums are present posterolabially and anterolingually. The A2 is an inflated subtriangular tooth with a conical main cusp in anterior position and a short anterior crest. The tooth is surrounded by a cingulum. A thickening of the cingulum is visible at the posterolingual corner. The P4 bears a small conical paracone and an enlarged, sharp, and curved postparacrista. The parastyle is connected by a thin crest to the base of the paracone. The protocone is low and triangular in cross-section. From the protocone extends a short lingual crest that ends freely close to the anterolingual border. A broad valley separates the protocone from the large, independent hypocone. A short hypoloph is attached to it. A ridge running parallel to the lingual margin is found lingually to the hypoloph.

The M1 bears a high metacone from which a regularly curved postmetacrista extends. The postparacrista is slightly longer than the premetacrista and the preparacrista. The preparacrista is connected to a hook-like parastyle. The protocone is

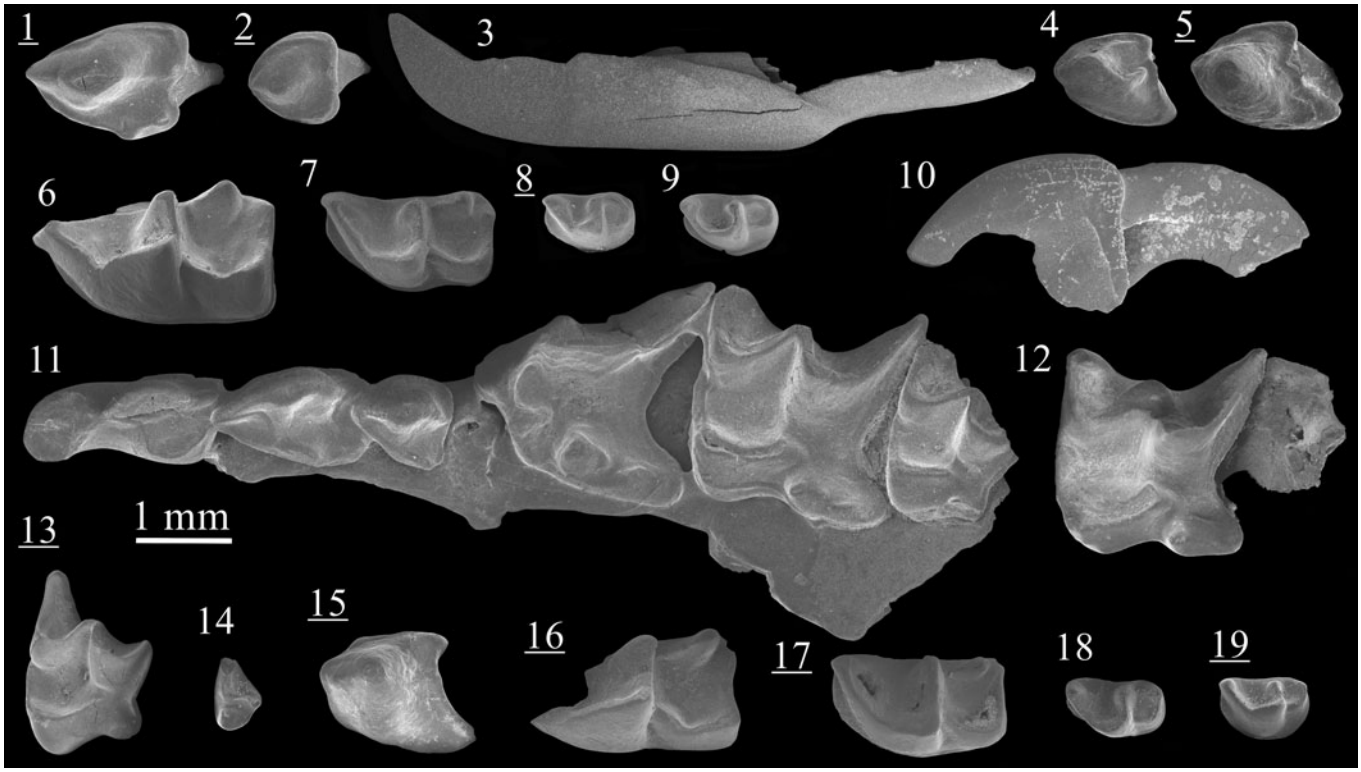

Figure 7. Scanning electron photomicrographs of *Crusafontina kormosi* from Triblavina (**1–9**) and Šalgovce 5 (**10–19**). (**1**) A1, TB170247; (**2**) A2, TB170256; (**3**) i1, TB170252, labial view; (**4**) a1, TB170255; (**5**) p4, TB170205; (**6**) m1, TB170223; (**7**) m2, TB170224; (**8**) m3, TB170228; (**9**) m3, TB170229; (**10**) I1, SG198253, labial view; (**11**) fragment of skull with I1–A2 and P4–M2, SG198262; (**12**) fragment of maxillary with M1, SG198291; (**13**) M2, SG198298; (**14**) M3, SG198308; (**15**) p4, SG198310; (**16**) m1, SG198350; (**17**) m2, SG198361; (**18**) m3, SG198390; (**19**) m3, SG198393. Images with underlined numbers are reversed.

https://doi.org/10.1017/jpa.2024.23 Published online by Cambridge University Press

low. The preprotocrista ends before reaching the base of the paracone. The postprotocrista is thicker posteriorly and delineates a broad, mortar-like trigon basin. A thin hypoloph is often distinguishable (two in KR, two in SG 5; Fig. 7.12). Alternatively, a short ridge with a thicker bulge, which is independent from the hypocone, is present (one in SG 5; Fig. 7.11). The M2 is reduced and shows a strong posterior compression, leading to a more trapezoid outline. The preparacrista is the longest labial crest. The parastyle is short, bladelike, and stands at an angle with the preparacrista. The hypocone is weak. In some cases, the hypocone only corresponds to a low bulge born by the lingual flange. The M3 is a vestigial, subtriangular element. Only a few structures are distinguishable: a labial S-shape crest including the protocone, a short preparacrista and postparacrista, a small posterolabial bulge (metacone?), a minute anterolingual protocone, and a flat posterolingual basin. These structures are only partly present in the single specimen from SG 5 (Fig. 7.14).

The height of the mandibular body is regular. The mandibular foramen is located below the anterior root of the m1. The two alveoli of m3 are well differentiated.

The i1 has a tip bent upward and slightly mesially (Fig. 7.3). This incisor is weakly bicuspulate; the posteriormost accessory cuspule is lower than the tip of the incisor. On the lingual side, the cingulum is distinguishable to absent. The a1 is a one-rooted, subtriangular tooth with a slightly laterally compressed cuspid in central position. The anterior cristid reaches the anterior margin. A thin bi-partitioned posterior cristid joins the broad posterior cingulid (Fig. 7.4). The posterolabial corner is more extended than the posterolingual one. The tooth is surrounded by a cingulid except for below the anterior cristid. The one-rooted p4 is robust and displays an uncompressed, high, and conical cuspid in slightly anterior position. The anterior crest is blunt. The posterolingual corner of the talon is extended.

The trigonid of m1 is significantly longer than the talonid. The bi-partitioned paralophid has a slight carnassial notch. The protoconid is bulbous. The metaconid is slightly higher than the paraconid. Both cuspids are close to each other, as they are in morphotype B (sensu Furió, 2007, fig. 5.13). The talonid is rectangular in shape. The weak entocristid and the oblique cristid are almost parallel. The entoconid is high and conical whereas the hypoconid is low and subtriangular. The entostylid is robust. Only a narrow cingulid is present, situated anterolabially. The m2 is overall a smaller version of the m1. The paralophid is slightly more oblique, the paraconid and metaconid are more separated, the anterior cingulid is stronger, and the entostylid is reduced. A small cuspule is found in the center of the talonid basin in one out of 12 specimens. The m3 is extremely small (Fig. 7.8, 7.9, 7.18, 7.19). The simple trigonid configuration is still preserved, despite the metaconid being smaller than the paraconid. The talonid displays a tiny basin surrounded by a continuous crest. The entoconid and the hypoconid are not distinct from the hypolophid.

Material.—See Table 5 for measurements. Triblavina: five I1, two A1, three A2, two P4, three M1, one M2, three i1, one a1, one p4, four m1, six m2, three m3, one fragment of mandible.

Krásno: six I1, four A1, one A2, 12 M1, five M2, 32 i1, one a1, one p4, eight m1, ten m2, two m3, one fragment of edentulous mandible.

Šalgovce 5: one fragment of maxillary with I1-A2 and P4-M2, eight I1, two A1, three A2, one fragment of maxillary with P4, three P4, one fragment of maxillary with M1, two M1, 10 M2, one M3, 14 i1, two a1, seven p4, nine m1, 17 m2, five m3, one fragment of edentulous mandible.

Remarks.—The specimens from Triblavina, Krásno, and Šalgovce 5 show clear similarities with *Crusafontina kormosi* from Kohfidisch. They display more advanced features than *C. endemica*: stronger centrocrista on A1, strengthening of the anterior cusps on P4, enlargement of M1, clear reduction of M2 and M3, broadening of the p4, and reduction of the Lm3/Lm1 ratio. Van Dam (2004) considered 0.40 as the Lm3/Lm1 ratio delimiting *C. endemica* from *C. kormosi*, which fits with the material from Triblavina (0.40) and Krásno (0.39).

Genus *Amblycoptus* Kormos, 1926

Type species.—*Amblycoptus oligodon* Kormos, 1926.

Other referred species.—*Amblycoptus topali* Jánossy, 1972; *A. jessiae* Doukas et al., 1995.

Occurrence.—*Amblycoptus* is identified from latest MN11 to MN16 of Europe (Jánossy, 1972; Rzebik-Kowalska, 1975; Doukas et al., 1995; Mészáros, 1996, 1997, 1998b; Van Dam, 2004; Doukas, 2005; Furió, 2007; Rzebik-Kowalska and Lungu, 2009; Vasileiadou and Doukas, 2022).

Amblycoptus jessiae Doukas et al., 1995
Figure 8

Holotype.—Fragment of right mandible with a1, p4–m2, AMPG MA 3296, Maramena, Greece (Doukas et al., 1995).

Diagnosis.—See Doukas et al. (1995, p. 54).

Occurrence.—MN13 of Greece (Doukas et al., 1995; Vasileiadou and Doukas, 2022), Spain (Van Dam, 2004; Furió, 2007), and Slovakia (this paper).

Description.—The massive I1 has a heavy, bent apex (Fig. 8.1). It is separated from the talon by a very slight notch. The talon is rounded in lateral view. The labial cingulum is especially thick below the notch. The A1 is an elongated, triangular tooth with a robust protocone in central position. The labial length of the tooth is slightly longer than the lingual one. A short anterior crest is attached to the independent parastyle. The paracone is found on the lingual side and is connected to the broad anterolingual cingulum. A weak (Fig. 8.2) to moderately strong (Fig. 8.3) hypocone is present posterior to the protocone. The A2 is a subtriangular and flat tooth that varies greatly in size (Fig. 8.4, 8.5). The main cusp is low and surrounded by a continuous and wide cingulum. A thin, central, posterior crest is often present (four out of six). A bulge is present lingually, in a relatively posterior position. The paracone of the P4 is massive. The parastyle is in a relatively anterior position and is much smaller than the protocone. A thin crest connects the parastyle to the base of

https://doi.org/10.1017/jpa.2024.23 Published online by Cambridge University Press

Table 5. Measurements (in mm) of *Crusafontina kormosi* from Triblavina (MN11), Krásno (MN11) and Šalgovce 5 (MN12), Slovakia. AW = anterior width; BL = labial length; H = height; L = length; LL = lingual length; LT = length of the talon; N = number of specimens; PE = length of the posterior emargination; PW = posterior width; TAW = talonid width; TRW = trigonid width; W = width.

Crusafontina kormosi, Triblavina

	I1			A1		A2		M1			i1	a1		p4	
	L	LT	H	L	W	L	W	PE	LL	AW	L	L	W	L	W
N	3	4	4	2	2	3	3	1	1	1	1	1	1	1	1
Min	2.47	1.06	1.67	1.74	1.22	0.93	0.93	—	—	—	—	—	—	—	—
Max	3.09	1.17	2.03	1.76	1.25	0.96	1.02	—	—	—	—	—	—	—	—
Mean	2.70	1.12	1.77	1.75	1.24	0.94	0.98	1.63	1.88	2.16	4.61	1.45	0.99	1.51	1.17
	m1			m2			m3								
	L	TRW	TAW	L	TRW	TAW	L	W							
N	2	3	3	2	2	3	3	3							
Min	2.33	1.16	1.12	1.62	0.89	0.88	0.94	0.57							
Max	2.43	1.22	1.25	1.75	0.96	0.97	0.96	0.59							
Mean	2.38	1.19	1.20	1.68	0.92	0.93	0.94	0.58							

Crusafontina kormosi, Krásno

	I1		A1	A2	M1			M2			i1		a1	
	LT	H	L	L	Bl	LL	AW	BL	LL	AW	L	H	L	W
N	3	4	2	1	1	1	1	1	1	1	1	13	2	2
Min	1.10	1.71	1.58	—	—	—	—	—	—	—	—	1.15	1.24	0.80
Max	1.27	1.83	1.60	—	—	—	—	—	—	—	—	1.37	1.39	0.86
Mean	1.18	1.76	1.59	1.09	1.19	2.01	2.23	1.06	0.92	1.79	4.94	1.22	1.31	0.83
	m1			m2			m3							
	L	TRW	TAW	L	TRW	TAW	L	W						
N	2	2	2	2	3	5	2	2						
Min	2.24	1.19	1.17	1.63	0.94	0.84	0.92	0.55						
Max	2.48	1.26	1.26	1.66	1.03	1.02	0.92	0.58						
Mean	2.36	1.23	1.23	1.64	1.00	0.91	0.92	0.56						

Crusafontina kormosi, Šalgovce 5

	I1			A1		A2		P4				M1				
	L	LT	H	L	W	L	W	BL	PE	LL	W	BL	PE	LL	AW	PW
N	1	5	7	3	3	4	4	3	4	4	4	2	2	2	3	3
Min	—	0.95	1.66	1.63	1.02	1.10	0.89	2.42	1.56	1.79	1.88	1.97	1.57	1.93	2.02	2.19
Max	—	1.19	1.83	1.71	1.05	1.26	1.03	2.55	1.73	1.96	2.25	2.25	1.77	2.20	2.05	2.25
Mean	2.25	1.11	1.75	1.67	1.03	1.18	0.97	2.50	1.65	1.85	2.08	2.11	1.67	2.06	2.03	2.21
	M2					M3		i1	p4		m1		m2			m3	
	BL	PE	LL	AW	PW	L	W	H	L	W	TRW	TAW	L	TRW	TAW	L	W
N	5	4	4	3	3	1	1	5	1	4	5	6	5	6	9	5	5
Min	1.20	1.08	1.15	1.80	1.03	—	—	1.27		1.23	1.09	1.18	1.77	0.97	0.86	0.88	0.58
Max	1.36	1.21	1.22	1.88	1.22	—	—	1.36		1.30	1.20	1.24	1.83	1.03	0.92	1.05	0.68
Mean	1.35	1.16	1.20	1.84	1.12	0.50	0.75	1.33	1.66	1.26	1.12	1.22	1.79	1.00	0.89	0.95	0.62

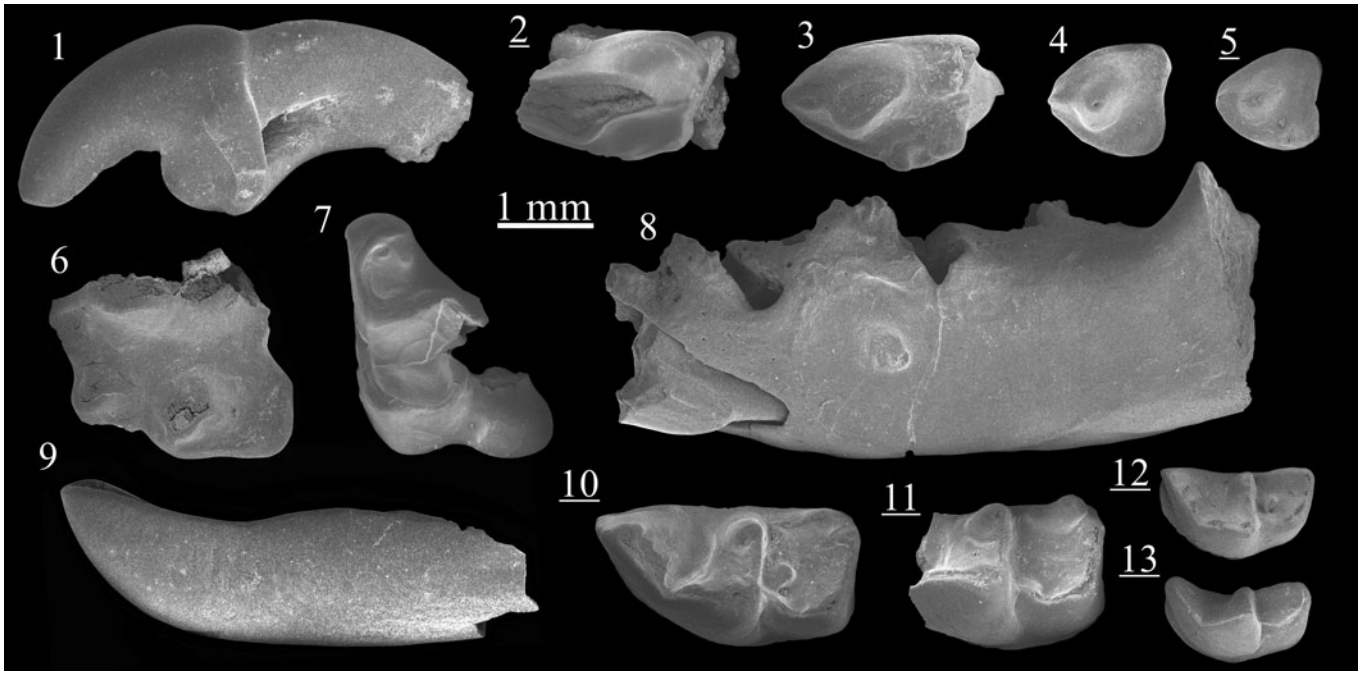

Figure 8. Scanning electron photomicrographs of *Amblycoptus jessiae* from Šalgovce 5. (**1**) I1, SG198150, labial view; (**2**) A1, SG198180; (**3**) A1, SG198183; (**4**) A2, SG198191; (**5**) A2, SG198192; (**6**) P4, SG198157; (**7**) M1, SG198158; (**8**) edentulous mandible, SG198247, labial view; (**9**) i1, SG198201, labial view; (**10**) m1, SG198220; (**11**) m1, SG198226; (**12**) m2, SG198232; (**13**) m2, SG198233. Images with underlined numbers are reversed.

https://doi.org/10.1017/jpa.2024.23 Published online by Cambridge University Press

the paracone. From the low protocone extends a preprotocrista and a short posterior crest. The hypocone is robust and independent. A short and blunt hypoloph is present, leading labially to the parastyle. The posterolingual flange is angular, with a discontinuous cingulum (Fig. 8.6). The posterior emargination is shallow.

The M1 has a massive labial complex with a low but robust preparacrista, postparacrista, and premetacrista. The parastyle is only slightly smaller than the protocone but stronger than all other cusps. The preparacrista and parastyle crest re-enter posterolingually as a hook. The mesostyle is situated lingually. The labial emargination is deep and reaches its maximum extent posteriorly to the mesostyle. The postmetacrista is straight. The paracone and metacone are similar. The preprotocrista and the postparacrista are sharp. The lingual margin is slightly concave. The hypocone is low and independent. There is no hypoloph, but there is a short anterolingually oriented prehypocrista.

The mandible is a massive element with seven alveoli, corresponding to the i1, one-rooted a1, one-rooted p4, two-rooted m1, and two-rooted m2. The alveolus of the p4 is enlarged in labial view. The posteriormost end of the alveolus of i1 is situated directly below the alveolus of the p4. The mandibular foramen is located slightly anterior to the posterior alveolus of the m1 (Fig. 8.8).

The i1 is acuspulate (Fig. 8.9). The apex is slightly bent upward. There is no visible cingulid. The a1 is a triangular element with a high and bulbous cuspid. The anterior cristid is extremely blunt. A short swelling is present at the posterolingual corner. The posterior crest is thin and almost straight. The p4 is only known from fragments. It displays a strong asymmetry as the labial side is much longer than the lingual one. The main cusp is very high, conical, and in anterior position. There is no distinct anterior crest. A thin posterior crest is present, joining lingually the oblique posterior cingulid.

The m1 is massive, with a trigonid longer than the talonid. The robust protoconid is connected to the paraconid by a long angular paralophid. The talonid bears a high, laterally compressed entoconid with a short entocristid. It is interrupted before the trigonid wall by a notch. The hypoconid is lower than the entoconid and has a broader base. The hypolophid is straight and leads to a small entostylid. In three specimens, the entostylid is found near the posterior margin, leading to a distinct postentoconid valley. In three other specimens, the entostylid is more anteriorly situated, leading to a very superficial valley. The oblique cristid is bent. In one specimen out of five, a short cristid is attached to the anterolingual section of the oblique cristid. In two other specimens, this short cristid leads to a relatively strong accessory cuspule at the anterolabial part of the talonid basin (Fig. 8.10). The labial cingulid is thin. The m2 is a relatively small molar. The paralophid is elongated and bi-partitioned. The paraconid is higher than the reduced metaconid. The talonid is square to rectangular. The entoconid is included within the entocristid. The hypoconid is well differentiated. The oblique cristid is parallel to the entocristid. The hypolophid is straight and ends as a low cusplet at the posterolingual corner. In unworn specimens, a short valley separates this cusplet from the entoconid. One out of seven specimens displays a robust accessory cuspule inside the talonid basin (Fig. 8.12). The narrow labial cingulid is either continuous or only present anteriorly.

Material.—See Table 6 for measurements. Šalgovce 5: five I1, 12 A1, six A2, five fragments of P4, five fragments of M1, 11 i1, six a1, one p4, 12 m1, seven m2, two edentulous mandibles.

Remarks.—Three species of large European Anourosoricini are identified in the late Neogene: *Amblycoptus oligodon* (MN11–MN13), *A. jessiae* (MN13), and *A. topali* (MN14–MN16). The m1/m2 ratio increases from the oldest to the youngest species because the m2 tends to become smaller. Doukas et al. (1995) identified a clear evolution of the posterolingual area in m1, as the entoconid, which is dominant in *A. oligodon*, is barely separated from the entostylid in *A. jessiae* and completely absorbed by it in *A. topali*. In the upper dentition, the A1 is smaller in *A. oligodon* than in *A. jessiae*. Both *A. jessiae* and *A. topali* also display a distinct parastyle on A1 (Doukas et al., 1995; Mészáros, 1996, 1997). Additionally, Mészáros (1997) observed an anterior displacement of the lingual cusp on A2 between *A. oligodon* and *A. topali*. On P4, the parastyle is situated relatively posteriorly in *A. topali*. The latter is also identified by the straight anterior, lingual and posterior margin of the P4 and M1. Finally, *A. topali* does not have A3, which is still present in *A. oligodon* according to Mészáros (1997).

The species from Šalgovce 5 shares strong morphological and morphometrical characteristics with *A. jessiae* from MN13 of Maramena (Doukas et al., 1995) and Las Casiones (Van Dam, 2004). Our material is distinct from *A. oligodon* by having a longer A1, a distinct parastyle on A1, a shallower postentoconid valley on m1, a relatively small m2, and by the punctual

Table 6. Measurements (in mm) of *Amblycoptus jessiae* from Šalgovce 5 (MN12), Slovakia. AW = anterior width; H = height; L = length; LL = lingual length; LT = length of the talon; N = number of specimens; PW = posterior width; TAW = talonid width; TRW = trigonid width; W = width.

	I1			A1		A2		M1		i1	p4		m1		
	L	LT	H	L	W	L	W	LL	AW	H	L	W	L	TRW	TAW
N	1	1	2	5	5	6	6	1	1	4	1	1	1	5	5
Min	—	—	2.15	2.20	1.32	1.06	1.09	—	—	1.41	—	—	—	1.47	1.43
Max	—	—	2.17	2.46	1.51	1.37	1.27	—	—	1.49	—	—	—	1.57	1.53
Mean	2.78	1.18	2.16	2.32	1.43	1.19	1.13	2.14	2.72	1.45	1.71	1.20	2.94	1.52	1.47
	m2														
	L	TRW	TAW												
N	2	4	5												
Min	1.65	0.86	0.70												
Max	1.81	1.04	0.91												
Mean	1.73	0.98	0.85												

https://doi.org/10.1017/jpa.2024.23 Published online by Cambridge University Press

presence of a cuspule on the talonid basin of m1–2. On the other hand, the frequency of hypocone on A1 and the usually superficial postentoconid valley on m1 are somewhat intermediate between *A. oligodon* and *A. jessiae*. This supports the interpretation that the material from Šalgovce 5 corresponds to a very early *A. jessiae*.

The presence of a minute cuspule inside the talonid basin of 2/5 m1 and 1/7 m2 (Fig. 8.10, 8.12) is an exceptional characteristic for an eulipotyphlan species. From a biomechanical point of view, this reduces the efficiency of the protocone/talonid mortar complex. Our material includes only a single M1 displaying a classic protocone, which limits the discussion. It is worth noting that a talonid cuspule is also present in one m2 of *Crusafontina kormosi* from Šalgovce 5 and in specimens from MN12 of Tardosbánya (Mészáros, 1998b, pl. 1, fig. 9.11).

Mészáros (1997) provided a thorough comparative study of both *A. oligodon* and *A. topali*, resulting in the inclusion of the last species within the new genus *Kordosia*. Additionally, Mészáros (1997) highlighted the very intermediate position of *A. jessiae*, considered in his work under the designation *Kordosia*? *jessiae*. Doukas (2005) argued that the main distinction between *Amblycoptus* and *Kordosia*, the loss of the A3, cannot be checked in the known material of *A. jessiae*. The presence of A3 in *A. oligodon* is only suggested by a tiny alveolus found in two maxillaries described by Kormos (1926, pl. III, fig. 1a vs. fig. 2). It appears that *A. oligodon*, *A. jessiae*, and *A. topali* belong to a single anagenetic lineage and that *A. topali* is not related to *Anourosex* (see Van Dam, 2010). No boundaries can be drawn separating these species, as shown by the early *A. jessiae* from Šalgovce 5 and the somewhat basal *A. topali* from Osztramos 1 (Mészáros, 1997, fig.5). A generic division is thus poorly justified. Consequently, *A. topali* is kept within *Amblycoptus*, as originally described by Jánossy (1972).

Tribe Nectogalini Anderson, 1879
Genus *Asoriculus* Kretzoi, 1959

Type species.—*Asoriculus gibberodon* (Petényi, 1864).

Other referred species.—*Asoriculus castellarini* (Pasa, 1947); *A. thenii* Malez and Rabeder, 1984; *A. maghrebensis* Rzebik-Kowalska, 1988; *A. burgioi* Masini and Sarà, 1998.

Diagnosis.—See Kretzoi (1959, p. 238), as "*Asoriculus* n. sg."

Occurrence.—*Asoriculus* is present from MN12 to the Early Pleistocene of Europe (Reumer, 1984; Mészáros, 1998b; Rzebik-Kowalska and Rekovets, 2016; Joniak et al., 2017; Moya-Costa et al., 2023).

Asoriculus gibberodon (Petényi, 1864)
Figure 9.1–9.5

Holotype.—Skull with right I1–M3 and left A3–M3, MÁFI Ob. 3685, Beremend, Hungary (Reumer, 1984).

Diagnosis.—See Reumer (1984, p. 94), under the name *Episoriculus gibberodon*.

Occurrence.—From MN12 to the Early Pleistocene (Reumer, 1984; Mészáros, 1998b; Furió, 2007; Joniak et al., 2017; Moya-Costa et al., 2023).

Description.—All teeth are slightly pigmented.

The A2? is elongated and asymmetrical. The pointy main cusp is included in a centrocrista, turning lingually at the anterior margin to join the lingual cingulum. The posterolingual corner is situated anterior to the posterolabial corner. The labial cingulum is similar to the lingual one. The single root is strongly oriented backward.

The long M1 has a W-shaped labial complex. The parastyle creates a hook with the short preparacrista at the anterolabial corner. The postmetacrista is elongated. The preprotocrista is very slightly curved and reaches the anterior flank of the paracone. The posterior part of the postprotocrista is split into two crests: one ends freely in the middle of the lingual area; the other touches the base of the strong metacone. A broad valley separates these anterolingual structures from the hypocone. A short posthypocrista is present, not connected to the continuous posterior cingulum (Fig. 9.2). This configuration of the short posthypocrista is thus intermediate between morphotypes A and B (sensu Reumer, 1984). The posterior emargination is strong. The M2 has a smaller dimension than the M1. The preparacrista, postparacrista, and premetacrista are relatively long, with the postmetacrista being still the longest labial crest. The connection between the postprotocrista and the base of the metacone is much weaker than on M1. The hypocone is clearly connected to the posterior cingulum (morphotype B; Fig. 9.3).

The p4 has a strong cuspid with a subtriangular base and is in a central position. A crest connects the cuspid to the anterior margin before turning lingually. The posterior crest has a posterolabial orientation before bending to the central part of the posterior border (Fig. 9.4). Narrow posterolingual and posterolabial cingulids are present.

The narrow trigonid of the m2 is as long as the trigonid. The paralophid is elongated and bi-partitioned. The paraconid is slightly projected anteriorly and is as high as the metaconid. The entoconid is high and pointy. The entocristid is very low. The oblique cristid connects the broad hypoconid to the posterolingual base of the protoconid. The hypolophid is slightly curved. The postentoconid valley is narrow. A continuous cingulid is present on the labial and posterior flank. In labial view, the anteriormost part of the cingulid slopes up. A faint lingual cingulid is visible.

Material.—Šalgovce 5: one A2? (L = 0.89, W = 0,70), one M1 (BL = 1.42, PE = 1.01, LL = 1.34, AW = 1.42, PW = 1.67), one M2 (BL = 1.19, PE = 1.02, LL = 1.28, PW = 1.52), one p4 (L = 1.12, W = 0.87), two m2 (L = 1.38, TRW = 0.79, TAW = 0.87; TAW = 0.81).

Remarks.—These specimens show clear nectogaline affinities. The combination of relatively small size, slightly pigmented teeth, slightly fissident I1, M1–2 with broad talon and a distinct hypocone, and m2 with a low entocristid are good indicators of *Asoriculus*. Our material fits the single Late Miocene *Asoriculus*, *A. gibberodon*, as described from

https://doi.org/10.1017/jpa.2024.23 Published online by Cambridge University Press

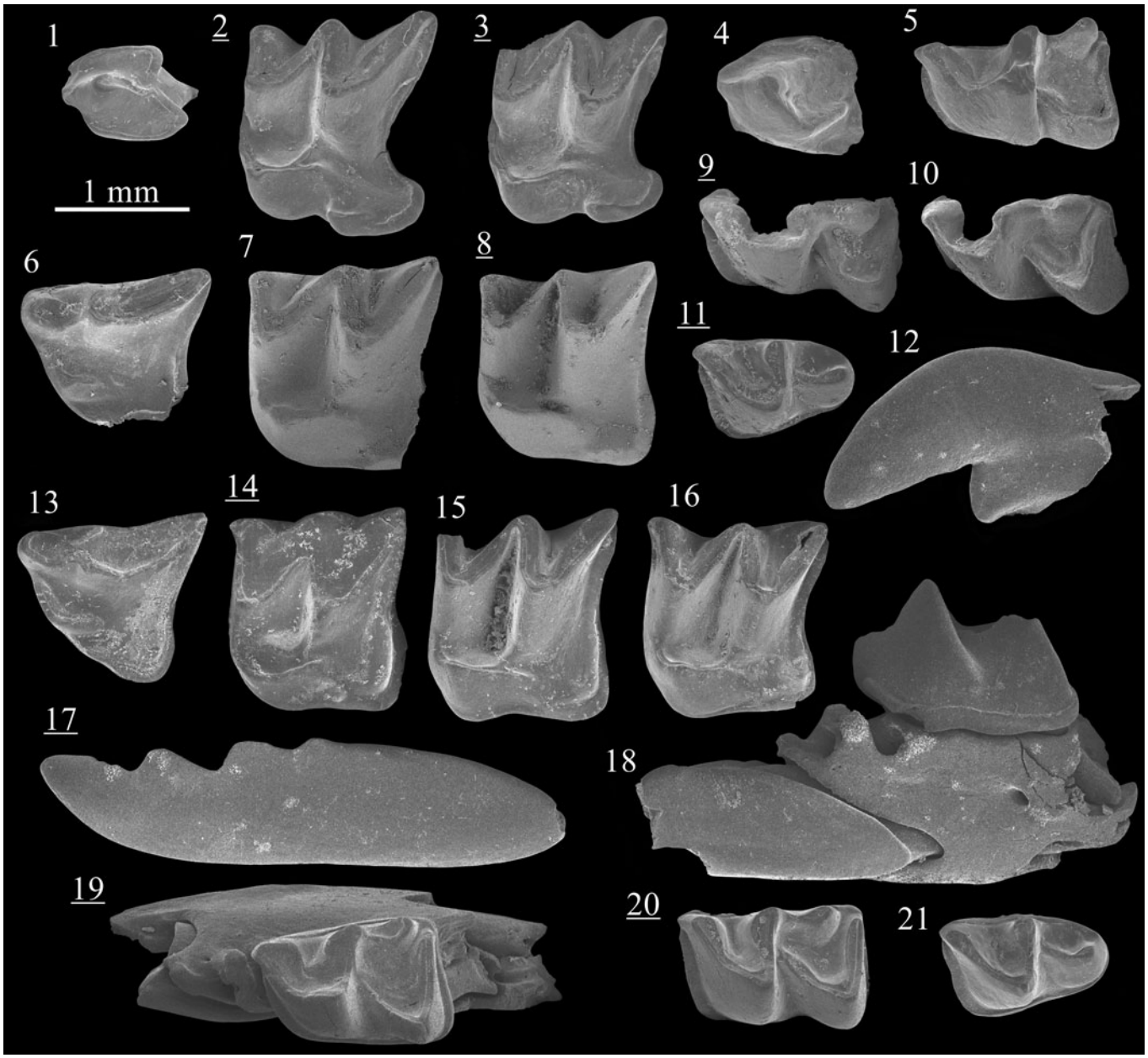

Figure 9. Scanning electron photomicrographs of *Asoriculus gibberodon* from Šalgovce 5 (**1–5**) and *Petenyia dubia* from Krásno (**6–11**) and Šalgovce 5 (**12–21**). (**1**) A2?, SG198601; (**2**) M1, SG198602; (**3**) M1, SG198603; (**4**) p4, SG198604; (**5**) m2, SG198601. (**6**) P4, KR127252; (**7**) M2, KR127253; (**8**) M2, KR127255; (**9**) m1, KR127278; (**10**) m2, KR127282; (**11**) m3, KR127292. (**12**) I1, labial view, SG198440; (**13**) P4, SG198450; (**14**) M1, SG198461; (**15**) M1, SG198463; (**16**) M2, SG198457; (**17**) i1, SG198494, labial view; (**18**) fragment of mandible with i1 and m1, SG198510, labial view; (**19**) fragment of mandible with m1, SG198511; (**20**) m2, SG198540; (**21**) m3, SG198574. Images with underlined numbers are reversed.

numerous localities (e.g., Reumer, 1984; Mészáros, 1998b; Furió, 2007).

The long stratigraphic range of *A. gibberodon* is a consequence of its broad morphological and morphometric variability. This motivated Reumer (1984) to synonymize *A. gibberodon* with *A. tornensis* Jánossy, 1972, and *A. borsodensis* Jánossy, 1972. According to Reumer (1984), the validity of *Asoriculus castellarini* also requires investigation. *Asoriculus* possibly occurs in the early Turolian of Moldova (Rzebik-Kowalska and Lungu, 2009) and Ukraine (Rzebik-Kowalska and Rekovets, 2016), under the denomination ?*Asoriculus* sp. and cf. *Asoriculus* sp., respectively. The specimens described from Popovo 3 (MN11) and Verkhnyaya Krynitsa 2 (MN11/12) by Rzebik-Kowalska and Rekovets (2016) display m1–2 with relatively high entocristid compared to *A. gibberodon*. The material from Šalgovce 5 and Tardosbánya (MN12; Mészáros, 1998b) does not display such distinctions and thus constitutes the oldest firm records of *A. gibberodon*, alongside the very limited simple from Vértesacsa, Hungary (?MN12; Joniak et al., 2017). At the same time, these mentions represent the earliest record of the Nectogalini.

The temporal distribution of *A. gibberodon* implies a longevity of at least 6 ma., which is high for a soricid species and likely the consequence of a reduced competition (see Van den

https://doi.org/10.1017/jpa.2024.23 Published online by Cambridge University Press

Hoek Ostende et al., 2023). This suggests that *A. gibberodon* was occupying one of the specialized niches of the Nectogalini, a tribe including semi-fossorial, semi-aquatic, and scansorial taxa (see He et al., 2010). *Asoriculus gibberodon* probably was using riparian environments as ecological corridors, so that the three locomotory reconstructions are plausible considering the lack of postcranial evidence.

Tribe Blarinellini Reumer, 1998
Genus *Petenyia* Kormos, 1934

Type species.—*Petenyia hungarica* Kormos, 1934.

Other referred species.—*Petenyia dubia* Bachmayer and Wilson, 1970; *P. katrinae* Qiu and Storch, 2000.

Diagnosis.—See Storch (1995, p. 230).

Occurrence.—*Petenyia* is recorded from the late Middle Miocene (Ziegler, 2003; Prieto, 2007), Late Miocene (Bachmayer and Wilson, 1970; Kordos, 1991; Mészáros, 1998b; Ziegler, 2006a; Furió et al., 2014; Rzebik-Kowalska and Rekovets, 2016), Pliocene (Storch and Qiu, 2000; Rzebik-Kowalska and Rekovets, 2016), and Pleistocene (Reumer, 1984) of Eurasia. The inclusion of *Petenyia dubia* within *Plioblarinella* (von Koenigswald and Reumer, 2020), which is not followed here, would restrict *Petenyia* to the Pliocene and Pleistocene.

Petenyia dubia Bachmayer and Wilson, 1970, and
Petenyia cf. *P. dubia* Bachmayer and Wilson, 1970
Figure 9.6–9.21

Holotype.—Fragment of left mandible with m1–3, NHMW 1970/1387, Kohfidisch, Austria (Bachmayer and Wilson, 1970).

Diagnosis.—See Reumer (1984, p. 66), under the name *Blarinella dubia*.

Occurrence.—From MN9 to MN14 of Europe (Bachmayer and Wilson, 1970; Mészáros, 1998b; Ziegler, 2006a; Furió, 2007) and MN10 to MN12 of Anatolia (Furió et al., 2014).

Description.—All teeth are moderately to strongly pigmented.

The I1 is strongly procumbent and elongated. The dorsal margin is weakly curved. The talon has a triangular outline in lateral view. The labial cingulum is oblique. The A1 has a low main cusp in anterior position and a centrocrista reaching the anterior and posterior border. A narrow cingulum surrounds the tooth, except for at the anterior border. The posterior section of the crest is slightly curved. The P4 has very high paracone and parastyle, which are connected by a sharp and short preparacrista. The high postparacrista is sharp and oblique. The protocone is visible on unworn specimens and included in the anterior V-shaped ridge. The preprotocrista marks the anterior central margin. The postprotocrista ends freely lingually to the paracone. The shallow basin is surrounded on the lingual and posterior border by a continuous ridge. The central part of the lingual ridge is thicker (hypocone).

On the quadrangular M1, the metacone and paracone are antero-posteriorly compressed. The preparacrista and premetacrista are short and parallel. The postparacrista and postmetacrista are longer and also parallel. A cingulum is present between the mesostyle and the metastyle. The anterolingual area is occupied by a U-shaped crest constituted by the preprotocrista, the protocone, and the free-ending postprotocrista. A thin crest connects the postprotocrista to the base of the metacone. The posterolingual corner bears a large hypoconal flange surrounded by a ridge. The M2 differs from the M1 only by its slightly smaller dimensions, the slightly more lingual position of the protocone, and the more rounded posterolingual margin (Fig. 9.14, 9.15 vs. Fig. 9.16).

The mandible has a straight ramus, and the incisor is almost parallel to it. Two broad aveoli are found between the i1 and the m1 (Fig. 9.18) corresponding to the a1 and the p4. The mental foramen is found below the talonid of the m1.

The i1 is tricuspulate and has a slightly bent apex cusp. The p4 is subtriangular and exaenodont. The main cuspid is connected to the pointy anterior margin by a thin ridge. A short, straight crest originates from the posterolingual flank of the cuspids and ends before joining the border. A bi-partitioned posterolabial crest connects the tip of the cuspid to the central posterior margin. A thin posterolingual cingulid is present.

The m1 is quadrangular. The paraconid has a triangular base and is included in a sharp, bi-partitioned paralophid. The metaconid is well developed and the metalophid is short. The trigonid valley is deep. On the posterior part, the entoconid is conical and connected to the flank of the metaconid by a high and straight entocristid. The oblique cristid is straight and is attached to the central part of the trigonid wall. The hypolophid ends abruptly at the posterolingual corner. The postentoconid valley is deep. A continuous cingulid is present all around the molar, except for directly below the paraconid. The m2 differs from the m1 by the more compressed trigonid, the less anterior direction of the paralophid, the more labial metaconid, and the wider metalophid. This leads to an even more rectangular outline. The m3 has an enlarged trigonid and reduced talonid. The paraconid and metaconid have the same height. The paralophid is straight. The talonid has a single cuspid, connected to the trigonid wall by a high cristid (Fig. 9.21). The cingulid surrounds all the m3 except for between the paraconid and the metaconid. The anterolabial section of the cingulid is thick.

Material.—See Table 7 for measurements. Studienka E (*P.* cf. *P. dubia*): one A1 (L = 0.99, W = 0.84), one M2 (Pe = 1.12, LL = 1.32, AW = 1.47), two m2 (L = 1.35, TRW = 0.85, TAW = 0.84).

Pezinok (*P.* cf. *P. dubia*): one M2 (BL = 1.35, PE = 1.19, LL = 1.30, TRW = 1.47, TAW = 1.52).

Triblavina (*P. dubia*): one I1 (L = 1.76, LT = 1.15, H = 1.04), one M1 (BL = 1.18, Pe = 1.06, LL = 1.12), one M2 (BL = 1.24), one M1/2 (BL = 1.33), one m1 (L = 1.35, TAW = 0.88), one m3.

Krásno (*P. dubia*): one I1, one P4, three M1, four M2, five M1/M2, six i1, six m1, 12 m2, one m1/m2, five m3.

Šalgovce 4 (*P.* cf. *P. dubia*): one fragment of m3.

Šalgovce 5 (*P. dubia*): nine I1, five P4, 11 M1, 10 M2, 11 i1, two p4, 20 m1, 22 m2, eight m3.

https://doi.org/10.1017/jpa.2024.23 Published online by Cambridge University Press

Table 7. Measurements (in mm) of *Petenyia dubia* from Krásno (MN11) and Šalgovce 5 (MN12), Slovakia. AW = anterior width; BL = labial length; H = height; L = length; LL = lingual length; LT = length of the talon; N = number of specimens; PE = length of the posterior emargination; PW = posterior width; TAW = talonid width; TRW = trigonid width; W = width.

Petenyia dubia, Krásno																
	P4	M1			M2					i1		m1		m2		
	BL	PE	LL	AW	BL	PE	LL	AW	PW	L	H	TRW	TAW	L	TRW	TAW
N	1	2	1	1	3	1	1	2	3	2	3	2	3	6	8	9
Min	—	1.16	—	—	1.28	—	—	1.28	1.41	3.56	0.95	0.80	0.76	1.33	0.67	0.82
Max	—	1.28	—	—	1.43	—	—	1.43	1.54	3.74	0.99	0.80	0.87	1.42	0.79	0.87
Mean	1.39	1.22	1.29	1.45	1.28	1.19	1.28	1.36	1.46	3.65	0.97	0.80	0.83	1.38	0.75	0.84
	m3															
	L	W														
N	4	5														
Min	1.09	0.66														
Max	1.12	0.75														
Mean	1.11	0.69														
Petenyia dubia, Šalgovce 5																
	I1			P4			M1					M2				
	L	LT	H	BL	LL	W	BL	PE	LL	AW	PW	BL	PE	LL	AW	PW
N	1	2	3	2	1	1	4	6	3	4	4	3	6	4	5	2
Min	—	1.01	1.29	1.41	—	—	1.31	1.25	1.36	1.47	1.45	1.25	1.08	1.21	1.39	1.42
Max	—	1.25	1.38	1.44	—	—	1.44	1.32	1.42	1.50	1.59	1.33	1.19	1.33	1.57	1.51
Mean	2.32	1.13	1.34	1.43	1.09	1.25	1.38	1.27	1.39	1.49	1.54	1.29	1.15	1.28	1.49	1.46
	i1		p4		m1			m2			m3					
	L	H	L	W	L	TRW	TAW	L	TRW	TAW	L	W				
N	2	6	1	1	12	15	18	7	6	17	5	7				
Min	3.87	0.88	—	—	1.37	0.76	0.79	1.26	0.85	0.73	1.09	0.66				
Max	3.89	0.96	—	—	1.50	0.96	0.97	1.54	0.95	1.00	1.25	0.81				
Mean	3.88	0.93	1.02	0.66	1.45	0.81	0.89	1.39	0.89	0.90	1.17	0.72				

Remarks.—These samples all display the diagnostic features of *Petenyia dubia*: the P4–M2 with a reduced posterolingual flank and with no posterior emargination, the P4 with protruding parastyle, the M1–2 with a freely ending postprotocrista and no hypocone, and the rectangular m1–2 with thick cingulids and high entocristid.

When describing the Late Miocene insectivores from Austria, Ziegler (2006a) considered the existence of *Petenyia* aff. *P. dubia* previous to and contemporaneous with the fauna of Kohfidisch, as several samples apparently have narrower lower molars. This statement is mainly based on the sample from Schernham. Other samples (Richardhof–Golfplatz, Richardhof–Wald, Eichkogel) have slightly smaller lower molars but do not show a clear change in the L/W ratio, which is also the case in the Slovak material. Additionally, the minor difference in size of the lower molars does not exceed 5% of the mean size of the type material, and the measurements of most lower molars are found within the variability of the material from Kohfidisch. Consequently, the material from Richardhof–Golfplatz, Richardhof–Wald, and Eichkogel is, alongside the main Slovak materials, attributed to *P. dubia* without reservation. The materials from Studienka E, Pezinok, and Šalgovce 4 are attributed to *P.* cf. *P. dubia* because of the limited sample size.

Discussion

Diversity pattern.—Soricidae represented a growing portion of the invertivore community during the Late Miocene. At least one species of Plesiosoricidae and eight species of Soricidae are identified in the Late Miocene of Slovakia (Table 8). They represent less than 25% of the eulipotyphlan material (number of identified specimens) from the Vallesian localities of Borský Svätý Jur (MN9), Studienka A (MN9), and Pezinok (MN10) (based on Cailleux et al., 2023, 2024; Cailleux,

Table 8. Composition of the Plesiosoricidae and Soricidae from the Late Miocene of Slovakia (number of identified specimens).

	MN9				MN10	MN11		MN12	
		Studienka						Šalgovce	
	Borský Svätý Jur	A	D	E	Pezinok	Triblavina	Krásno	4	5
Plesiosoricidae									
Plesiosorex evolutus	2								
Soricidae									
Paenelimnoecus repenningi		13				5	14		
Paenesorex bicuspis	80	18	1 (cf.)						
Isterlestes aenigmaticus n. gen. n. sp.									27
Crusafontina endemica	60	16							
Crusafontina kormosi						35	83		86
Amblycoptus jessiae									76
Asoriculus gibberodon									6
Petenyia dubia				4	1 (cf.)	8	44	1 (cf.)	101

https://doi.org/10.1017/jpa.2024.23 Published online by Cambridge University Press

unpublished data). In the Turolian of Triblavina (MN11) and Krásno (MN11), soricids represent more than 60% of the material, ultimately reaching around 78% of the material in Šalgovce 5 (MN12). This trend is also apparent in eastern Austria where soricids reach around 20% of the eulipotyphlan material in Vallesian localities and 45% in Eichkogel (MN11) (based on Daxner-Höck et al., 2016, supplementary data). The differences found between eastern Austrian and Slovak data from roughly contemporaneous localities (e.g., Krásno and Eichkogel) are explained by difference in methodology, since the fragmented materials of soricid species, notably the lower incisors, housed at the NHMW were more frequently discarded by Ziegler (2006a). The increase of soricids frequency coincides with the extinction of the Heterosoricidae (Cailleux, unpublished data) and Dimylidae and with the overall decline of the Erinaceidae (Cailleux et al., 2023).

Apart from possible orbital forcing (Harzhauser et al., 2004), the early Turolian turnover of the Eulipotyphlan fauna in Slovak basins is mainly explained by the relatively fast change from lacustrine-type and forested wetland environments to riparian environments (Daxner-Höck et al., 2016; Cailleux et al., 2024) following the southern retreat of Lake Pannon (Joniak et al., 2020). This coincided with a time of global change in the mammal communities of Europe, related to the progressive settlement of seasonality (Franzen and Storch, 1999), which is already well documented in southwestern Europe during the Vallesian (e.g., Casanovas-Vilar et al., 2014). It is likely that Lake Pannon was playing a role in the maintenance of large, moistened environments in the northern part of the Pannonian realm, somehow tempering and delaying less-favorable habitats. The following spatial reduction of favorable environments for Eulipotyphla provides a suitable explanation for the decline of the territorial fossorial talpids (Cailleux et al., 2024). Like nowadays (e.g., Cross, 1985), woodland and riparian buffers favor soricids in both abundance and diversity. Simultaneously, reduced diversity of the other Eulipotyphla likely participated in the wider eco-morphological spectrum of Turolian soricids.

Pannonian realm as source area for Soricidae.—The strategic position of Slovakia in Europe and its very favorable Late Miocene environmental parameters made the region both an efficient migratory corridor and a source area for insectivore species, as exemplified by the very high diversity and abundance of insectivore taxa in central Europe (Ziegler, 2006a; Furió et al., 2011; Daxner-Höck et al., 2016; Sabol et al., 2021; Cailleux et al., 2023, 2024) and already demonstrated by Van Dam (2004) for the Anourosoricini. Several soricid species found in Slovakia are widespread in Europe. This is the case for *Paenelimnoecus repenningi*, *Crusafontina endemica*, *Crusafontina kormosi*, and *Petenyia dubia* (e.g., Ziegler, 2006b; Furió, 2007). The genus *Paenesorex* is restricted to southern Germany, Slovakia, and Hungary (Ziegler, 2003; Hír et al., 2017), which constitute an area of high insectivore diversity during the Vallesian of Europe (based on Ziegler, 2006b; Furió et al., 2011). *Asoriculus gibberodon*, the oldest Nectogalini, was widespread during the Early Pliocene (e.g., Reumer, 1984; Moya-Costa et al., 2023), but the earliest mentions of this species are found in the late Turolian of Slovakia and Hungary (i.e., in the Danube basin [Šalgovce 5] and in the margins of the adjacent Transdanubian Central Range [Tardosbánya and Vértesacsa]) (Mészáros, 1998b; Joniak et al., 2017). *Isterlestes* n. gen. is for now only known from the Danube basin, so it is uncertain if this genus is endemic or if its small size and low abundance make it hard to identify in late Turolian localities.

The first Late Miocene occurrences (MN9) of *Paenesorex* and the discovery of *Isterlestes* n. gen. (MN12) complete the Late Miocene record of the Soricini, previously represented by *Zelceina* in Mikhailovka 2 (MN11) and Verkhnya Krynitsa 2 (MN11/12; Rzebik-Kowalska and Rekovets, 2016), and by *Deinsdorfia* in Maramena (MN13; Doukas et al., 1995). The materials from these localities are strongly distinct from each other, making it clear that the Soricini were already well diversified before the Pliocene, despite these records showing a limited spatial distribution in Europe. Curiously, *Zelceina* is also recorded in Ertemte, China (MN13; Storch, 1995), making its biogeographic history puzzling.

The *Amblycoptus* species from Šalgovce 5 displays clear affinities with *A. jessiae*, which at first sight is unexpected from a chronological and geographical perspective. This species is identified only in MN13 localities of Spain and Greece and is also suspected in Kavurca, Anatolia (MN13-14; Engesser, 1980; Van Dam, 2004), whereas *A. oligodon* is identified in slightly older deposits from the Pannonian basins. Until now, *Amblycoptus oligodon* also was the only form co-occurring with the more ancestral *Crusafontina*, as in the contemporaneous Hungarian fauna of Tardosbánya 3/1 (MN12; Mészáros, 1998b). The presence of transitional features in the material from Šalgovce 5 strongly supports that this locality contains the oldest occurrence of *A. jessiae*.

The paleobiogeography of the Anourosoricini tribe in Europe is strewn with phases of geographic expansion and contraction (Van Dam, 2004). These phases are correlated with periodic variation of precipitation. The model of Van Dam (2004) supports the idea that southern European regions corresponded to sink areas, whereas the source area of Anourosicini was in higher latitudes. This model is very much in line with the observed continuous and abundant presence of Anourosoricini in the Late Miocene of central Europe. The presence of *Amblycoptus jessiae* was recorded from both Greek and Spanish deposits correlated to MN13. Based on the previous model, this strongly supports that *A. jessiae* is actually a migrant from the northern regions (i.e., the northern Pannonian realm). At the same time, the mentioned model perfectly illustrates the spectrum of tolerance of soricid taxa towards drier environments during the Late Miocene, as this family contains taxa with high (e.g., *Paenelimnoecus*, *Petenyia*), moderate (e.g., *Asoriculus*, *Crusafontina*, *Amblycoptus*), and low (e.g., *Paenesorex*, *Isterlestes* n. gen.) drought tolerance.

Acknowledgments

We would like to express our deep gratitude to G. Cuenca-Bescós and L. Voyta for their valuable comments on the manuscript. The editorial assistance provided by J. Calede and J. Kastigar was also greatly appreciated. We are very grateful to U.B. Göhlich and E. Robert for their help

https://doi.org/10.1017/jpa.2024.23 Published online by Cambridge University Press

providing comparative material from the paleontological collections of Vienna and Lyon. We are also thankful to J. Religa-Sobczyk for providing pictures of several Soricidae from the collection of the Institute of Systematics and Evolution of Animals of the Polish Academy of Sciences. We extend our thanks to L. Li who provided bibliographic resources and M. Furió for his suggestions on *Amblycoptus* and *Kordosia*. This research was supported by grants UK/27/2022 and UK/221/2023 of Comenius University, the Scientific Grant Agency of the Ministry of Education, Science, Research and Sport of the Slovak Republic and Slovak Academy of Sciences (VEGA) under the contract VEGA 1/0533/21, the Slovak Research and Development Agency (projects APVV-20-0120 and APVV-20-0079), and the Austrian Science Funds (FWF) under the project P-15724-N06.

Declaration of competing interests

The authors declare none.

Data availability statement

Data available from the Dryad Digital Repository: http://doi.org/10.5061/dryad.8cz8w9gzv.

References

Anderson, J., 1879, Anatomical and Zoological Research: Comprising an Account of the Zoological Results of the Two Expeditions to Western Yunnan in 1866 and 1875; and a Monograph of the Two Cetacean Genera *Platanista* and *Orcella*: London, Bernard Quaritz, v. 1/2, 985 p.

Bachmayer, F., and Wilson, R.W., 1970, Die Fauna der altpliozänen Höhlen-und Spaltenfüllungen bei Kohfidisch, Burgenland (Österreich) small mammals (Insectivora, Chiroptera, Lagomorpha, Rodentia) from the Kohfidisch Fissures of Burgenland, Austria: Annalen des Naturhistorischen Museums in Wien, v. 74, p. 533–587.

Bannikova, A.A., Chernetskaya, D., Raspopova, A., Alexandrov, D., Fang, Y., Dokuchaev, N., Sheftel, B., and Lebedev, V., 2018, Evolutionary history of the genus *Sorex* (Soricidae, Eulipotyphla) as inferred from multigene data: Zoologica Scripta, v. 47, p. 518–538, https://doi.org/10.1111/zsc.12302.

Baudelot, S., 1972, Etude des chiroptères, insectivores et rongeurs du Miocène de Sansan (Gers) [Ph.D. thesis]: Toulouse, France, Université Paul Sabatier, 380 p.

Bown, T.M., 1980, The fossil Insectivora of Lemoyne Quarry (Ash Hollow Formation, Hemphillian), Keith County, Nebraska: Transactions of the Nebraska Academy of Sciences and Affiliated Societies, v. 8, p. 99–122.

Burgin, C.J., Colella, J.P., Kahn, P.L., and Upham, N.S., 2018, How many species of mammals are there?: Journal of Mammalogy, v. 99, p. 1–14, https://doi.org/10.1093/jmammal/gyx147.

Cailleux, F., Joniak, P., and van den Hoek Ostende, L.W., 2023, The Late Miocene Erinaceidae (Eulipotyphla, Mammalia) from the Pannonian region, Slovakia: Journal of Paleontology, v. 97, p. 777–798, https://doi.org/10.1017/jpa.2023.50.

Cailleux, F., Joniak, P., and Van den Hoek Ostende, L.W., 2024, The Late Miocene Talpidae (Eulipotyphla, Mammalia) from the Pannonian region, Slovakia: Journal of Paleontology, v. 98, p. 128–151, https://doi.org/10.1017/jpa.2023.95.

Casanovas-Vilar, I., Van den Hoek Ostende, L.W., Furió, M., and Madern, P.A., 2014, The range and extent of the Vallesian Crisis (Late Miocene): new prospects based on the micromammal record from the Vallès–Penedès basin (Catalonia, Spain): Journal of Iberian Geology, v. 40, p. 29–48, http://dx.doi.org/10.5209/rev_JIGE.2014.v40.n1.44086.

Crochet, J.Y., and Green, M., 1982, Contributions à l'étude des micromammifères du gisement Miocène supérieur de Montredon (Hérault): 3 – Les insectivores: Palaeovertebrata, v. 12, p. 119–131.

Cross, S.P., 1985, Responses of small mammals to forest riparian perturbations, *in* Johnson, R.R., Ziebell, C.D., Patton, D.R., Folliot, P.F., and Hamre, R.H., eds. Riparian Ecosystems and Their Management: Reconciling Conflicting Uses: Proceedings of the First North American Riparian Conference, Tucson, Arizona, USA, April 16–18, 1985, U.S. Forest Service General Technical Report RM-GTR-120, Fort Collins, Colorado, USA, p. 269–275.

Daxner-Höck, G., Harzhauser, M., and Göhlich, U.B., 2016, Fossil record and dynamics of Late Miocene small mammal faunas of the Vienna Basin and adjacent basins, Austria: Comptes Rendus Palevol, v. 15, p. 855–862, https://doi.org/10.1016/j.crpv.2015.06.008.

de Blainville, H.M.D., 1838, Ostéographie des mammifères insectivores. In: de Blainville, H.M.D., Ostéographie ou description iconographique comparée du squelette et du système dentaire des mammifères récents et fossiles pour servir de base à la zoologie et à la géologie: Livraison 6, Paris, J. B. Baillière et Fils, v. 4., 115 p.

Doben-Florin, U., 1964, Die Spitzmause aus dem Alt-Burdigalium von Wintershof-West bei Eichstatt in Bayern: Abhandlungen, Bayerische Akademie der Wissenschaften, Mathematisch-Naturwissenschaftliche Klasse, Neue Folge, v. 117, p. 1–82.

Doukas, C.S., 2005, Greece, *in* Van den Hoek Ostende, L.W., Doukas, C.S., and Reumer, J.W.F., eds., The Fossil Record of the Eurasian Neogene Insectivores (Erinaceomorpha, Soricomorpha, Mammalia), Part I: Scripta Geologica Special Issue, v. 5, p. 99–112.

Doukas, C.S., Van den Hoek Ostende, L.W., Theocharopoulos, C., and Reumer, J.W.F., 1995, Insectivora (Erinaceidae, Talpidae, Soricidae, Mammalia), *in* Schmidt-Kittler, N., ed. The vertebrate locality Maramena (Macedonia, Greece) at the Turolian–Ruscinian boundary: Münchner Geowissenschaftliche Abhandlungen, v. A28, p. 43–64.

Engesser, B., 1972, Die obermiozäne Säugetierfauna von Anwil (Baselland): Tätigkeitsberichte der Naturforschenden Gesellschaft Baselland, v. 28, p. 37–363.

Engesser, B., 1980, Relationships of some insectivores and rodents from the Miocene of North America and Europe: Bulletin of Carnegie Museum of Natural History, v. 14, p. 1–68.

Engesser, B., 2009, The insectivores (Mammalia) from Sansan (Middle Miocene, southwestern France): Schweizerische Paläontologische Abhandlungen, v. 128, p. 1–91.

Engesser, B., and Storch, G., 2008, Latest Oligocene Didelphimorphia, Lipotyphla, Rodentia and Lagomorpha (Mammalia) from Oberleichtersbach, Rhön Mountains, Germany: Courier Forschungsinstitut Senckenberg, v. 260, p. 185–251.

Fejfar, O., 1966, Die Plio-Pleistozänen Wirbeltierfaunen von Hajnacka und Ivanovce (Slowakei, CSSR); V. *Allosorex stendus* n. gn. sp. aus Ivanovce A: Neues Jahrbuch für Geologie und Paläontologie, Abhandlungen, v. 123, p. 221–248.

Fejfar, O., Storch, G., and Tobien, H., 2006, Gundersheim 4, a third Ruscinian micromammalian assemblage from Germany: Palaeontographica Abteilung A, v. 278, p. 97–111, https://doi.org/10.1127/pala/278/2006/97.

Fejfar, O., von Koenigswald, W., and Sabol, M., 2020, *Allosorex stenodus* Fejfar, 1966 (Eulipotyphla, Soricidae): re-description of type material and re-interpretation of its fossil record: Fossil Imprint, v. 76, p. 84–98, https://doi.org/10.37520/fi.2020.006.

Fischer, G., 1814, Volumen tertium. Quadrupedum reliquorum, cetorum et monotrymatum descriptionem continens. Zoognosia tabulis synopticis illustrata: Mosquae, Nicolai Sergeidis Vsevolozsky, 734 p.

Franzen, J.L., and Storch, G., 1999, Late Miocene mammals from central Europe. *in* Agustí, J., Rook, L., and Andrews, O., eds., Hominoid Evolution and Climatic Change in Europe: Cambridge, UK, Cambridge University Press, v. 1, p. 165–190.

Franzen, J.L., Fejfar, O., and Storch, G, 2003, First micromammals (Mammalia, Soricomorpha) from the Vallesian (Miocene) of Eppelsheim, Rheinhessen (Germany): Senckenbergiana Lethaea, v. 83, p. 95–102.

Furió, M., 2007, Los Insectívoros (Soricomorpha, Erinaceomorpha, Mammalia) del Neógeno Superior del Levante Ibérico [Ph.D. thesis]: Universitat Autònoma de Barcelona, Spain, 341 p.

Furió, M., and Mein, P., 2008, A new species of *Deinsdorfia* (Soricidae, Insectivora, Mammalia) from the Pliocene of Spain: Comptes Rendus Palevol, v. 7, p. 347–359.

Furió, M., Casanovas-Vilar, I., and Van den Hoek Ostende, L.W., 2011, Predictable structure of Miocene insectivore (Lipotyphla) faunas in Western Europe along a latitudinal gradient: Palaeogeography, Palaeoclimatology, Palaeoecology, v. 304, p. 219–229, https://doi.org/10.1016/j.palaeo.2010.01.039.

Furió, M., Van Dam, J., and Kaya, F., 2014, New insectivores (Lipotyphla, Mammalia) from the Late Miocene of the Sivas Basin, Central Anatolia: Bulletin of Geosciences, v. 89, p. 163–181, https://doi.org/10.3140/bull.geosci.1472.

Gibert, J., 1975, New insectivores from the Miocene of Spain: Proceedings van de Koninklijke Nederlandse Akademie van Wetenschappen, v. 78, p. 108–133.

Green, M., 1977, A new species of *Plesiosorex* (Mammalia, Insectivora) from the Miocene of South Dakota: Neues Jahrbuch für Geologie und Paläontologie Monatshefte, v.4, p. 189–198.
Gunnel, G.F., Bown, T.M., Hutchson, J.H., Bloch, J.I., 2008, Lipotyphla, *in* Janis, C.M., Gunnell, G.F., and Uhen, M.S., eds., Evolution of Tertiary Mammals of North America, Volume 2: Cambridge, UK, Cambridge University Press, p. 89–125, https://doi.org/10.1017/CBO9780511541438.008.
Hall, E.R., 1929, A second new genus of hedgehog from the Pliocene of Nebraska: University of California, Publications in Geological Sciences, v. 18, p. 227–231.
Harzhauser, M., Daxner-Höck, G., and Piller, W.E., 2004, An integrated stratigraphy of the Pannonian (Late Miocene) in the Vienna Basin: Austrian Journal of Earth Sciences, v. 95, p. 6–19.
He, K., Li, Y.J., Brandley, M.C., Lin, L.K., Wang, Y.X., Zhang, Y.P., and Jiang, X.L., 2010, A multi-locus phylogeny of Nectogalini shrews and influences of the paleoclimate on speciation and evolution: Molecular Phylogenetics and Evolution, v. 56, p. 734–746.
Heller, F., 1930, Eine forest-bed-fauna aus der Sackdillinger Höhle (Oberpfalz): Neues Jahrbuch für Mineralogie, Geologie und Paläontologie. Abhandlungen. Abteilung B, Geologie, Paläontologie, v. 63, p. 247–298.
Hinton, M.A.C., 1911, The British fossil shrews: Geological Magazine, v. 8, p. 529–539.
Hír, J., Venczel, M., Codrea, V., Angelone, C., van den Hoek Ostende, L.W., Kirscher, U., and Prieto, J., 2016, Badenian and Sarmatian s. str. from the Carpathian area: overview and ongoing research on Hungarian and Romanian small vertebrate evolution: Comptes Rendus Palevol, v. 15, p. 863–875.
Hír, J., Venczel, M., Codrea, V., Rössner, G.E., Angelone, C., van den Hoek Ostende, L.W., Rosina, V.V., Kirscher, U., and Prieto, J., 2017, Badenian and Sarmatian s.str. from the Carpathian area: taxonomical notes concerning the Hungarian and Romanian small vertebrates and report on the ruminants from the Felsőtárkány Basin: Comptes Rendus Palevol, v. 16, p. 312–332, https://doi.org/10.1016/j.crpv.2016.11.006.
Hofmann, A., 1892, Beiträge zur miozänen Säugetierfauna der Steiermark: Jahrbuch der Kaiserlich Königlichen Geologischen Reichsanstalt, Wien, v. 42, p. 63–76.
Hugueney, M., Mein, P., and Maridet, O., 2012, Revision and new data on the Early and Middle Miocene soricids (Soricomorpha, Mammalia) from central and south-eastern France: Swiss Journal of Palaeontology, v. 131, p. 23–49.
Jánossy, D., 1972, Middle Pliocene microvertebrate fauna from the Osztramos Loc. 1. (Northern Hungary): Annales Historico-naturales Musei Nationalis Hungarici, v. 64, p. 27–52.
Jin, C.-Z., and Kawamura, Y., 1997, A new species of the extinct shrew *Paenelimnoecus* from the Pliocene of Yinan, Shandong Province, northern China: Paleontological Research, v. 1, p. 67–75.
Joniak, P., 2005, New rodent assemblages from the Upper Miocene deposits of the Vienna Basin and Danube Basin [Ph.D. thesis]: Department of Geology and Paleontology, Faculty of Natural Sciences, Comenius University in Bratislava, Slovakia, 126 p.
Joniak, P., 2016, Upper Miocene rodents from Pezinok in the Danube Basin, Slovakia: Acta Geologica Slovaca, v. 8, p. 1–14.
Joniak, P., and Šujan, M., 2020, Systematic and morphometric data of Late Miocene rodent assemblage from Triblavina (Danube Basin, Slovakia): Data in Brief, v. 28, e104961, https://doi.org/10.1016/j.dib.2019.104961.
Joniak, P., Hír, J., Šujan, M., and Mészáros, L., 2017, Small mammals from Vértesacsa as a contribution to chronology of the Late Miocene Zagyva Formation (W Hungary): Acta Geologica Slovaca, v. 9, p. 15–24.
Joniak, P., Šujan, M., Fordinál, K., Braucher, R., Rybár, S., Kováčová, M., Kováč, M., and AsterTeam, 2020, The age and paleoenvironment of a Late Miocene floodplain alongside Lake Pannon: rodent and mollusk biostratigraphy coupled with authigenic $^{10}Be/^{9}Be$ dating in the northern Danube Basin of Slovakia: Palaeogeography, Palaeoclimatology, Palaeoecology 538, e109482, https://doi.org/10.1016/j.palaeo.2019.109482.
Kerr, R., 1792. Class I. Mammalia: containing a complete systematic description, arrangement, and nomenclature, of all the known species and varieties of the Mammalia, or animals which give suck to their young: London and Edinburgh, A. Strahan and T. Cadell and W. Creech, 644 p.
Kordikova, E.G., 2000, Insectivora (Mammalia) from the Lower Miocene of the Aktau Mountains, south-eastern Kazakhstan: Senckenbergiana Lethaea, v. 80, p. 67–79.
Kordos, L., 1991, Le *Rudapithecus hungaricus* de Rudabánya, Hongrie: L'Anthropologie, v. 95, p. 343–362.
Kormos, T., 1926, *Amblycoptus oligodon* n. g. & n. sp. Új cickány-féle a magyarországi pliocénból. [Eine neue Spitzmaus aus dem ungarischen Pliozän]: Annales Historico Naturales Musei Nationalis Hungarici, v. 24, p. 352–370.
Kormos, T., 1934, Neue Insektenfresser, Fledermause und Nager aus dem Oberpliozan der Villanyer Gegend: Földtani Közlöny, v. 64, p. 296–321.
Kretzoi, M., 1959, Insectivoren, Nagetiere und Lagomorphen der jungstpliozanen Fauna von Csarnota im Villanyer Gebirge (Sudungarn): Vertebrata Hungarica, v. 1, p. 237–246.
Li, L. 2022. New species of *Plesiosorex* (Eulipotyphla) from the middle Miocene of Gansu: the first record of Plesiosoricidae in China: Historical Biology, v. 35, p. 1556–1563, https://doi.org/10.1080/08912963.2022.2102912.
Linnaeus, C., 1766, Systema Naturae per Regna Tria Naturae (twelfth edition), tome 1, Regnum Animale: Stockholm, Laurentii Salvii, 824 p.
Malez, M., and Rabeder, G., 1984, Neues Fundmaterial von Kleinsäugern aus der altpleistozänen Spaltenfüllung Podumci 1 in Norddalmatien (Kroatien, Jugoslawien): Beiträge zur Paläontologie von Österreich, v. 11, p. 439–510.
Martin, L.D., and Lim, J.D., 2004, A new species of *Plesiosorex* (Mammalia, Insectivora) from the Early Miocene of Nebraska, USA: Neues Jahrbuch für Geologie und Paläontologie-Monatshefte, v. 3, p. 129–134, https://doi.org/10.1127/njgpm/2004/2004/129.
Masini, F., and Sarà, M., 1998, *Asoriculus burgioi* sp. nov. [Soricidae, Mammalia] from the Monte Pellegrino faunal complex [Sicily]: Acta Zoologica Cracoviensia, v. 41, p. 111–124.
Mayr, H., and Fahlbusch, V., 1975, Eine unterpliozäne Kleinsäugerfauna aus der Oberen Süsswasser-Molasse Bayerns: Mitteilungen der Bayerischen Staatssammlung für Paläontologie und Historische Geologie, v. 15, p. 91–111.
Ménouret, B., and Mein, P., 2008, Les vertébrés du Miocène supérieur de Soblay (Ain, France): Travaux et Documents des Laboratoires de Géologie de Lyon, v. 165, p. 3–97.
Mészáros, L.G., 1996, Soricidae (Mammalia, Insectivora) remains from three Late Miocene localities in western Hungary: Annales Universitatis Scientiarum Budapestinensis de Rolando Eötvös Nominatae-Sectio Geologica, v. 31, p. 5–25.
Mészáros, L.G., 1997, *Kordosia*, a new genus for some Late Miocene Amblycoptini shrews (Mammalia, Insectivora): Neues Jahrbuch für Geologie und Paläontologie–Monatshefte, v. 2, p. 65–78.
Mészáros, L.G., 1998a, *Crusafontina* (Mammalia, Soricidae) from Late Miocene localities in Hungary: Senckenbergiana Lethaea, v. 77, p. 145–159.
Mészáros, L.G., 1998b, Late Miocene Soricidae (Mammalia) fauna from Tardosbánya (Western Hungary): Hantkeniana, v. 2, p. 103–125.
Mészáros, L.G., 1999, Some insectivore (Mammalia) remains from the Late Miocene locality of Alsótelekes (Hungary): Annales Universitatis Scientiarum Budapestinensis de Rolando Eötvös Nominatae-Sectio Geologica, v. 32, p. 35–47.
Minwer-Barakat, R., García-Alix, Martin-Suárez, E., and Freudenthal, M., 2010, Soricidae (Soricomorpha, Mammalia) from the Pliocene of Tollo de Chiclana (Guadix Basin, southern Spain): Journal of Vertebrate Paleontology, v. 30, p. 535–546, https://doi.org/10.1080/02724631003622001.
Moya-Costa, R., Cuenca-Bescós, G., and Rofes, J., 2023, The shrews (Soricidae, Mammalia) of the early and middle Pleistocene of Gran Dolina (Atapuerca, Spain): reassessing their paleontological record in the Iberian Peninsula: Quaternary Science Reviews, v. 309, e108093, https://doi.org/10.1016/j.quascirev.2023.108093.
Oshima, M., Tomida, Y., and Orihara, T., 2017, A new species of *Plesiosorex* (Mammalia, Eulipotyphla) from the Early Miocene of Japan: first record of the genus from East Asia: Fossil Imprint, v. 73, p. 292–299, https://doi.org/10.2478/if-2017-0016.
Pasa, A., 1947, I mammiferi di alcune antiche brecce Veronesi: Memorie del Museo Civico di Storia Naturale di Verona, v. 1, p. 1–111.
Petényi, S.J., 1864, Hátrahagyott munkái: Magyar Tudományos Akademia Kiadása, Pest, v. 1, p. 1–130.
Pipík, R., and Sabol, M., 2005, *Paenelimnoecus* sp. (Lipotyphla, Mammalia) from the Late Miocene deposits of the Turiec Basin (Slovakia) and its paleoenvironment: Beiträge zur Paläontologie, v. 29, p. 15–21.
Pomel, N.A., 1848, Études sur les carnassiers insectivores. I. Insectivores fossiles. II. Classification des insectivores: Archives des Sciences Physiques et Naturelles v. 9, p. 159–165, 244–251.
Prieto, J., 2007, Kleinsäuger-Biostratigraphie und Paläoökologie des höheren Mittelmiozäns (MN 8) Bayerns: Spaltenfüllungen der Fränkischen Alb und Lokalitäten der Oberen Süßwassermolasse im Vergleich [Ph.D. thesis]: Ludwig Maximilian University, München, Germany, 213 p.
Prieto, J., and Van Dam, J.A., 2012, Primitive Anourosoricini and Allosoricinae from the Miocene of Germany: Geobios, v. 45, p. 581–589, https://doi.org/10.1016/j.geobios.2012.03.001.
Qiu, Z., and Storch, G., 2000, Die unterpliozäne kleinsäugerfauna von bilike, Innere Mongolei, China (Mammalia: Lipotyphla, Chiroptera, Rodentia, Lagomorpha): Senckenbergiana Lethaea, v. 80, p. 173–229.
Reumer, J.W.F., 1984, Ruscinian to Early Pleistocene Soricidae (Insectivora, Mammalia) from Tegelen (The Netherlands) and Hungary: Scripta Geologica, v. 73, p. 1–173.

Reumer, J.W.F., 1992, The taxonomical position of the genus *Paenelimnoecus* Baudelot, 1972 (Mammalia: Soricidae): a resurrection of the subfamily Allosoricinae: Journal of Vertebrate Paleontology, v. 12, p. 103–106.
Reumer, J.W.F., 1998, Classification of the fossil and recent shrews, *in* Wójcik, J.M., and Wolsan, M., eds., Białowieża: Mammal Research Institute, Polish Academy of Science, p. 5–22.
Rzebik-Kowalska, B., 1975, The Pliocene and Pleistocene insectivores (Mammalia) of Poland. II. Soricidae: *Paranourosorex* and *Amblycoptus*: Acta Zoologica Cracoviensia v. 20, p. 167–182.
Rzebik-Kowalska, B., 1988, Soricidae (Mammalia, Insectivora) from the Plio-Pleistocene and Middle Quaternary of Morocco and Algeria: Folia Quaternaria, v. 57, p. 51–90.
Rzebik-Kowalska, B., 1991, Pliocene and Pleistocene insectivores (Mammalia) of Poland. VIII. Soricidae. *Sorex* Linnaeus, 1758, *Neomys* Kaup, 1829, *Macroneomys* Fejfar, 1966, *Paenelimnoecus* Baudelot, 1972 and Soricidae indeterminata: Acta Zoologica Cracoviensia, v. 34, p. 323–424.
Rzebik-Kowalska, B., and Lungu, A., 2009, Insectivore mammals from the Late Miocene of the Republic of Moldova: Acta Zoologica Cracoviensia – Series A: Vertebrata, v. 52, p. 11–60, https://doi.org/10.3409/azc.52a_1-2.11-60.
Rzebik-Kowalska, B., and Nesin, V.A., 2010, Erinaceomorpha and Soricomorpha (Insectivora, Mammalia) from the Late Miocene of Ukraine: Krakow, Institute of Systematics and Evolution of Animals, Polish Academy of Sciences, 61 p.
Rzebik-Kowalska, B., and Rekovets, L.I., 2016, New data on Eulipotyphla (Insectivora, Mammalia) from the Late Miocene to the Middle Pleistocene of Ukraine: Palaeontologia Electronica, v. 19, 19.1.9A, https://doi.org/10.26879/573.
Sabol, M., Joniak, P., Bilgin, M., Bonilla-Salomón, I., Cailleux, F., Čerňanský, A., Malíková, V., Šedivá, M., and Tóth, C., 2021, Updated Miocene mammal biochronology of Slovakia: Geologica Carpathica, v. 72, p. 425–443, https://doi.org/10.31577/GeolCarp.72.5.5.
Schinz, H.R., 1837, Verzeichnis der in der Schweiz vorkommenden Wirbelthiere: Neue Denkschriften der Allgemeinen Schweizerischen Gesellschaft für die Gesammten Naturwissenschaften, v. 1, p. 1–165.
Schötz, M., 1989, Die *Plesiosorex*-Funde (Insectivora, Mammalia) aus der Kiegsgrube Maßendorf (Obere Süßwassermolasse Niederbayerns): Mitteilungen der Bayerischen Staatssammlung für Paläontologie und Historische Geologie, v. 29, p. 141–157.
Seemann I., 1938, Die Insektenfresser, Fledermäuse und Nager aus der obermiocänen Braunkohle von Viehhausen bei Regensburg: Palaeontographica A, v. 898, p. 1–55.
Storch, G., 1995, The Neogene mammalian faunas of Ertemte and Harr Obo in Inner Mongolia (Nei Mongol), China, 11. Soricidae (Insectivora): Senckenbergiana Lethaea, v. 75, p. 221–251.
Storch, G., and Qiu, S., 1991, Insectivores (Mammalia: Erinaceidae, Soricidae, Talpidae) from the Lufeng hominoid locality, Late Miocene of China: Geobios, v. 24, p. 601–621.
Sulimski, A., 1959, Pliocene insectivores from Węże: Acta Palaeontologica Polonica, v. 4, p. 119–173.
Sulimski, A., 1962, Supplementary studies on the insectivores from Weze 1 (Poland): Acta Palaeontologica Polonica, v. 7, p. 441–498.
Šujan, M., Braucher, R., Kováč, M., Bourlčs, D. L., Rybár, S., Guillou, V., and Hudáčková, N., 2016, Application of the authigenic $^{10}Be/^{9}Be$ dating method to Late Miocene–Pliocene sequences in the northern Danube Basin (Pannonian Basin System): confirmation of heterochronous evolution of sedimentary environments: Global and Planetary Change, v. 137, p. 35–53, https://doi.org/10.1016/j.gloplacha.2015.12.013.
The NOW Community, 2023, New and Old Worlds Database of Fossil Mammals (NOW). Licensed under CC BY 4.0. Retrieved [10.08.2023] from https://nowdatabase.org/now/database/. https://www.doi.org/10.5281/zenodo.4268068.
Van Dam, J.A., 2004, Anourosoricini (Mammalia: Soricidae) from the Mediterranean region: a pre-Quaternary example of recurrent climate-controlled north–south range shifting: Journal of Paleontology, v. 78, p. 741–764, https://doi.org/10.1666/0022-3360(2004)078<0741:AMSFTM>2.0.CO;2.
Van Dam, J.A., 2010, The systematic position of Anourosoricini (Soricidae, Mammalia): paleontological and molecular evidence: Journal of Vertebrate Paleontology, v. 30, p. 1221–1228, https://doi.org/10.1080/02724634.2010.483553.
Van den Hoek Ostende, L.W., 2001, Insectivore faunas from the Lower Miocene of Anatolia – Part 6: Crocidosoricinae (Soricidae): Scripta Geologica, v. 122, p. 47–81.
Van den Hoek Ostende, L.W., Furió, M., and Garcia-Paredes, I., 2009, New data on *Paenelimnoecus* from the middle Miocene of Spain support the shrew subfamily Allosoricinae: Acta Palaeontologica Polonica, v. 54, p. 159–164, https://doi.org/10.4202/app.2009.0117.
Van den Hoek Ostende, L.W., Joniak, P., Rojay, B., Aten, C., Bilgin, M., and Pelaez-Campomanes, P., 2019, Early Miocene insectivores of Gökler (Kazan Basin, Central Anatolia, Turkey): Palaeobiodiversity and Palaeoenvironments, v. 99, p. 701–722, https://doi.org/10.1007/s12549-019-00396-1.
Van den Hoek Ostende, L.W., Bilgin, M., Braumuller, Y., Cailleux, F., and Skandalos, P., 2023, Live long and prosper? Assessing longevity of small mammal taxa using the NOW Database, *in* Casanovas-Vilar, I., Van den Hoek Ostende, L.W., Janis, C.M., Saarinen, J., eds., Evolution of Cenozoic Land Mammal Faunas and Ecosystems: 25 Years of the NOW Database of Fossil Mammals. Vertebrate Paleobiology and Paleoanthropology (VERT): Cham, Switzerland, Springer International Publishing, p. 111–129, https://doi.org/10.1007/978-3-031-17491-9_8.
Van Valen, L., 1966, Deltatheridia, a new order of Mammals: Bulletin of the American Museum of Natural History, v. 132, p. 5–126.
Vasileiadou, K., and Doukas, C.S., 2022, The fossil record of insectivores (Mammalia: Eulipotyphla) in Greece, *in* Vlachos, E., ed., Fossil Vertebrates of Greece Vol. 2: Laurasiatherians, Artiodactyles, Perissodactyles, Carnivorans, and Island Endemics: Cham, Switzerland, Springer, p. 33–92, https://doi.org/10.1007/978-3-030-68442-6_3.
Viret, J., 1940, Étude sur quelques Erinacéidés fossiles (suite) – Genres *Plesiosorex*, *Lanthanotherium*: Laboratoire de Geologie de l'Universitéde Lyon, v. 39, p. 31–67.
Viret, J., and Zapfe, H, 1952, Sur quelques Soricidés Miocènes: Eclogae Geologicae Helvetiae, v. 44, p. 411–426.
von Koenigswald, W., Reumer, J., 2020, The enamel microstructure of fossil and extant shrews (Soricidae and Heterosoricidae, Mammalia) and its taxonomical significance: Palaeontographica A, v. 316, p. 79–164, https://doi.org/10.1127/pala/2020/0095.
Von Zimmermann, E.A.W., 1778–1783, Geographische Geschichte des Menschen, und der allgemein verbreiteten vierfussigen Thiere, nebst einer Hieher gehorigen zoologischen Weltcharte. Vol. 2. Geographische Geschichte des Menschen, und der vierfussigen Thiere. Zweiter Band. Enthalt ein vollstandiges, Verzeichniss aller bekannten Quadrupeden: Weygandschen Buchhandlung, Leipzig, 276 p.
Waddell, P.J., Okada, N., and Hasegawa, M., 1999, Towards resolving the interordinal relationships of placental mammals: Systematic Biology, v. 48, p. 1–5.
Wilson, R.W., 1960, Early Miocene rodents and insectivores from northeastern Colorado: University of Kansas Paleontological Contributions, Article 24, Vertebrata 7, p. 1–92, http://hdl.handle.net/1808/3798.
Winge, H., 1917, Udsigt over Insekternes indbyrdes Slægtskab: Videnskabelige Meddelelser fra Dansk Naturhistorisk Forening i Kjøbenhavn, v. 68, p. 83–203.
Zazhigin, V.S., and Voyta, L.L., 2022, New Neogene anourosoricin shrews from northern Asia: Palaeontologia Electronica, v. 25, 25.3.a29, https://doi.org/10.26879/1209.
Ziegler, R., 2003, Shrews (Soricidae, Mammalia) from Middle Miocene karstic fissure fill sites of Petersbuch near Eichstätt, southern Franconian Alb (Bavaria): Paläontologische Zeitschrift, v. 77, p. 303–322.
Ziegler, R., 2005, The insectivores (Erinaceomorpha and Soricomorpha, Mammalia) from the Late Miocene hominoid locality Rudabánya: Palaeontographia Italica, v. 90, p. 53–81.
Ziegler, R., 2006a, Insectivores (Lipotyphla) and bats (Chiroptera) from the Late Miocene of Austria: Annalen des Naturhistorischen Museums in Wien, Serie A für Mineralogie und Petrographie, Geologie und Paläontologie, Anthropologie und Prähistorie, v. 1, p. 93–196.
Ziegler, R., 2006b, Miocene insectivores from Austria and Germany—an overview: Beiträge zur Paläontologie, v. 30, p. 481–494.

Accepted: 12 March 2024